FORSCHUNGSZENTRUM JÜLICH GmbH

KFA

Institut für Angewandte Werkstofforschung

Measurement of Neutron Flux in the AVR

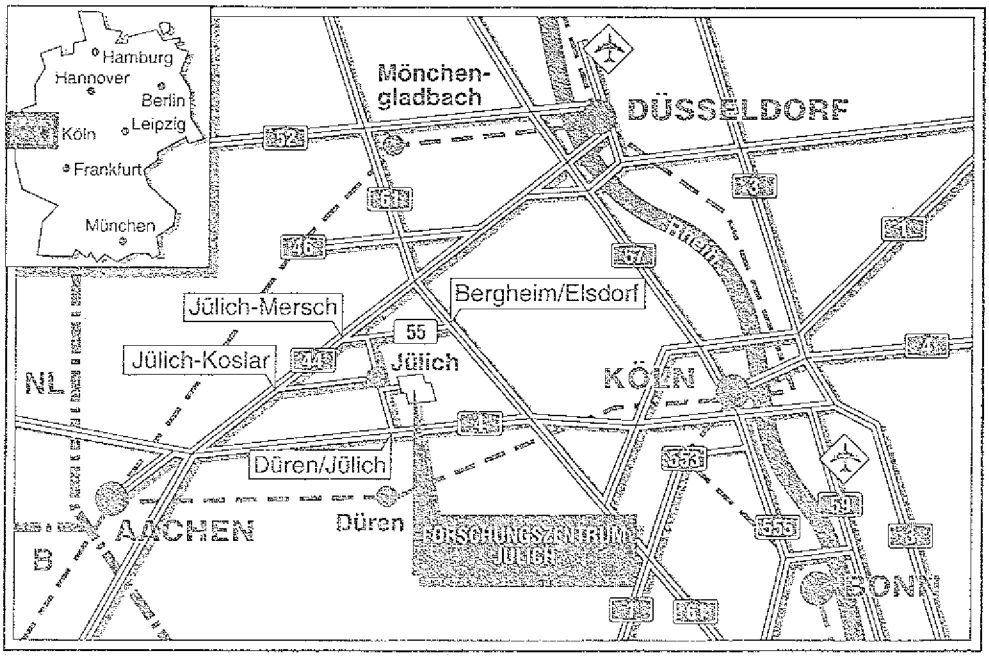

Berichte des Forschungszentrums Jülich ; 2467
ISSN 0366-0885
Institut für Angewandte Werkstofforschung Jül-2467

Zu beziehen durch: Forschungszentrum Jülich GmbH · Zentralbibliothek
Postfach 1913 · D-5170 Jülich · Bundesrepublik Deutschland
Telefon: 02461/61-6102 · Telefax: 02461/61-6103 · Telex: 833556-70 kfa d

Measurement of Neutron Flux in the AVR

H. Yamagishi, N. Wakayama, H. Itoh, K. Sakasai
Japan Atomic Energy Research Institute
H. Brixy, J. Oehmen, R. Hecker
Forschungszentrum Juelich GmbH
H.-J. Hantke
Energietechnik

Measurement of Neutron Flux in the AVR*

H.Yamagishi, N.Wakayama, H.Itoh, K.Sakasai
Reactor Instrumentation Laboratory
Japan Atomic Energy Research Institute
Tokai-mura, Naka-gun, Ibaraki-ken, 319-11 Japan

H.Brixy, J.Oehmen, R.Hecker
Institut fuer Angewandte Werkstofforschung
Forschungszentrum Juelich GmbH
D-5170 Juelich 1, Federal Republic of Germany

H.Hantke
Energietechnik
Am Poeglschlag 21, D-8080 Fuerstenfeldbruck,
Federal Republic of Germany

Abstract

The experiment to measure neutron flux distribution in the steam generator built above the reactor core of the high temperature gas-cooled reactor (AVR) in the Federal Republic of Germany was carried out by using new type High Temperature In-core Fission Counter-chambers (HTICs) and Wide Range Neutron Flux Measuring Electronics (WRMEs) in December 1988.

In the experiment, three HTICs were installed into the pipe of the steam generator. They operated properly to measure neutron flux from reactor start-up to full power without interference noise. Dynamic change of the neutron flux at each position of HTICs due to reactor power-change was able to be measured on real time from reactor start-up to full power.

---

* This work was carried out in cooperation between Japan Atomic Energy Research Institute Tokai, Japan and Forschungszentrum Juelich, Germany.

1. Introduction

Until recent years there was no in-core fission counter-chamber which could be used to measure neutron flux in a wide range at very high temperature (higher than 600° C). Accordingly it was impossible to measure neutron flux in a wide range in the reactor vessel of HTGRs on real time. Then Japan Atomic Energy Research Institute (JAERI) developed a High Temperature In-core Fission Counter-chamber (HTIC) which had a measurement range of 8 decades for neutron flux and a maximum operating temperature of 800° C.

JAERI wanted a demonstration test of the HTIC in an actual high temperature gas-cooled reactor. Forschungszentrum Juelich (KFA) needed to measure neutron flux distribution in the steam generator (SG) which was built above the reactor core of Arbeitsgemeinschaft Versuchsreaktor (AVR) in order to verify neutron flux computed in 1968. JAERI and KFA made a plan to measure neutron flux distribution in the SG of the AVR as a joint experiment. This experiment was carried out as HTA-10, one of the final verification tests for safety performance of the AVR, in December 1988.

Outline of the AVR is as follows. The AVR was constructed by Hochtemperatur-Reaktorbau GmbH (HRB) in the Federal Republic of Germany and reached initial criticality in 1966. The reactor is a high temperature gas-cooled reactor of the graphite-moderated, helium-gas-cooled and pebble-bed type. The reactor has steam generators built above the core in the reactor vessel. The full reactor thermal power, maximum outlet gas temperature and full electric power are 46MW, 950° C and 15MW, respectively.

The technical data and construction of the AVR are shown in Table 1.1 and Fig. 1.1.

2. Performances of HTIC and Electronics

The single neutron flux measuring system which was used for the AVR experiment consists of the HTIC, a heat-resistant signal cable, a wideband preamplifier and the WRME. The performances are as follows.

2.1 Performance of HTIC

The HTIC was developed for HTGRs as a neutron sensor for commissioning tests such as initial critical tests, power-up tests and neutron flux mapping in the reactor vessel. The HTIC is an in-core counter-chamber which operates at high temperature and has a wide measurement range for neutron flux. The HTIC operates in pulse-counting and Mean Square Voltage measuring (MSV, Campbelling) modes at 800° C as well as at room temperature and has a measurement range of 8 decades of neutron flux from 10^2 to 10^{10} n/cm^{2}s.

Table 2.1 and Fig. 2.1 show the specifications and the structure of the HTIC. The outside diameter and neutron sensitive length of the HTIC are 10mm and 80mm. The HTIC has one Mineral Insulated cable (MI-cable) with heat-resistance to 900° C. The outside diameter of the MI-cable is 5mm.

Special features of the HTIC are as follows; 95%Xe+N_2 mixture gas is used as ionization gas to improve operating performance at high temperature. The adoption of 95%Xe+N_2 mixture gas permits the realization of a fission counter-chamber which operates in lower pressure (2 atm abs.) of ionized gas and lower applied voltage (100 V) as compared with that of a conventional fission counter with Ar+N_2 mixture gas. Moreover Xe+N_2 mixture gas produces large current output pulses (1.6μA) with short electron collection time (100ns). To ensure heat-resistance up to 800° C, the pressure vessel (outer electrode) and the inner electrode of HTIC are made of a nickel alloy (Hastelloy-X). A special metal-ceramic seal, which is heat-resistant to 800° C, is used for the terminal of signal MI-cable in order to prevent gas travelling in the chamber and the insulator of MI-cable.

2.2 Nuclear electronics

To obtain the wide measurement range for neutron flux using pulse-counting and MSV method, a wideband preamplifier with a frequency band-width of "4KHz-13MHz" was fabricated to amplify neutron signals from the HTIC. The preamplifier, which operates in current pulse mode, has input impedance of 50 ohm, output impedance of 50 ohm (93 ohm for MSV channel) and gain of 14K ohm equivalent.

The Wide Range Neutron Measuring Electronics (WRME) consisted of a pulse-counting channel, a MSV measuring channel, a wide range output circuit and a period amplifier. The WRME was developed as the nuclear electronics of a wide range power monitoring system for HTGRs. The wide range power monitoring system, which consists of a High Temperature Fission Counter-chamber, a Push-pull preamplifier and the WRME, is able to cover the start-up range, intermediate range and power range for power monitoring of HTGRs. A demonstration test of the wide range power monitoring systems was carried out in the AVR from December 1987 to December 1988.

Figs. 2.2 and 2.3 show a schematic block diagram and a front panel view of the WRME. The WRME covers the measurement range of 10 decades for neutron flux and also makes a reactor period indication.

2.3 Preparation test in the JRR-4

The neutron flux measuring system was tested in the JRR-4 to measure the output linearities as a function of neutron flux. In the test, the output linearities, plateau curves and noises were measured under the conditions of room temperature and 800° C.

The results of output linearity measurements are shown in Fig. 2.4. By the test in the JRR-4, it was confirmed that the neutron flux measuring system has an output linearity for a neutron flux range of 8 decades from 2×10^2 to 2×10^{10} n/cm^{2}s under temperature conditions at

800°C as well as at room temperature.

3. Calibration of neutron sensitivity

Three HTICs (#1, #2 and #3) were fabricated for the AVR experiment. The calibrations of their neutron sensitivities were undertaken in Japan before shipment to KFA. Fig. 3.1 shows dimensions of the graphite pile which was used for calibrations of neutron sensitivities. Two neutron sources (Am-Be, 3.7×10^{11}Bq x 2) were inserted into the graphite pile. The HTICs were calibrated by using a known standard BF_3 counter. The calibration of the BF_3 counter was carried out in the standard neutron field of a national laboratory at the Ministry of International Trade and Industry in Japan.

In the calibration test of HTICs, the standard BF_3 counter and the HTICs were alternately put at the side of the graphite pile and neutron pulse counts of each detector were measured. The neutron sensitivity of each HTIC was calculated from the sensitivity of the BF_3 counter.

By the calibration test, neutron sensitivities of 0.0068, 0.0070 and 0.0068 cps/nv were found out for HTIC#1(Serial No. FA-1-31), HTIC#2(FA-1-32) and HTIC#3(FA-1-33), respectively. Fig. 3.2 shows the outside dimensions of HTIC#1, #2 and #3. The results of examinations of HTIC#1 to #3 are shown in Tables 3.1, 3.2 and 3.3.

In the plan of installing the HTICs into the AVR, it was decided that the HTICs were to be covered with a heat-resistant Al_2O_3 braiding sheath in order to insulate them from grounding of the AVR structure. The Al_2O_3 braiding sheath has a thickness of 1mm and contains 14% B_2O_3 (by weight) as a neutron absorber. The neutron sensitivities of HTIC#1, #2 and #3 covered with Al_2O_3 braiding sheath were also measured. They were 0.0052, 0.0054 and 0.0052 cps/nv, respectively.

4. Installation of HTICs and electronics in the AVR

In the AVR experiment, it was planned that three HTICs and seven thermocouples were to be installed into the reactor vessel by using a vertical steam generator pipe as a guide tube. The inside diameter of the steam generator pipe was 20mm. The HTICs and the thermocouples were assembled with a penetration flange to seal reactor pressure. Fig. 4.1 shows a composition of HTICs assembled for the AVR experiment. Fig. 4.2 also shows the distance from the penetration flange to the top of each sensor. The completed assembly is shown in Photos. 4.1 to 4.7. The signal cables of HTICs were connected to penetration cables at the inside of the seal flange by using special connectors which were heat-resistant to 350°C. Figs. 4.3 to 4.6 show the detailed structure of the seal flange with penetration cables and a penetration rig. Photo. 4.8

shows the completed assembly being carried from KFA to the AVR.

Fig. 4.7 shows the positions of HTICs and electronics installed in the AVR plant, and Fig. 4.8 shows the detailed positions of HTICs and thermocouples in the SG. The sensitive part of HTIC#1 was fixed at 1091mm above the lowest position of the SG. The positions of HTIC#2 and #3 were also fixed at 2653mm and 4156mm. In Fig. 4.8, arrow marks show measurement positions of thermocouples.

As shown in Fig. 4.7, the electronics for neutron flux measuring were installed in an instrument room which was at the outside of the reactor containment. The signal cables between the seal flange and the wideband preamplifiers were laid on a cable tray in the containment by using Teflon-insulated triaxial cables. The length of each Teflon-cable was 35m. The total length of signal cable between HTIC#1 and the preamplifier was approximately 45m.

Photo. 4.9 shows the wideband preamplifier installed on the outside wall of the reactor containment, and Photo. 4.10 shows the WRMEs mounted on the rack in the instruments room of the AVR.

5. Adjustment of the Neutron Flux Measuring System

5.1 Composition of the Neutron Flux Measuring System

Fig. 5.1 shows the block diagram of the neutron flux measuring system which was used in the AVR experiment. Three HTICs were installed into the pipe of the SG which was built above the reactor core of the AVR. Each measuring channel was named channel#1, #2 and #3 in the order of HTIC position nearest to the reactor core.

The electronics of channel#1 was composed of the wideband preamplifier, the signal divider and the WRME which had the pulse-counting channel and MSV measuring channel. Channel#1 was able to cover neutron flux measurement in the range from $2x10^2$ to $2x10^{10}$ n/cm^2s.

The composition of channel#2 was the same as that of channel#1. Channel#3 had a pulse-counting channel only because it had been expected that the neutron flux density at HTIC#3 position would not be over the measurement range of pulse-counting channel even at full power operation of the AVR. Channel#3 covered the neutron flux measuring range from $2x10^2$ to $2x10^8$ n/cm^2s.

5.2 Cable connection and system noise

Due to the restrictions of the AVR design, each signal cable between HTIC and preamplifier had to be a long cable of about 45m. In addition to this each signal line had four connections. After the reactor start-up, it was impossible to repair or adjust the cables and ground connections because no-one could enter the reactor containment. The ground connections of the signal line were very important to cut out the influences of field noises.

All cable connections between the HTICs and the end of the signal cables were inspected by using a pulse reflection method and perfect connections were confirmed. Also it was confirmed that the insulation resistances of cables were sufficient. System noises were inspected at the output of the wideband preamplifier by using an oscilloscope. Interference noises for neutron measurement were observed. Therefore the ground connection for the outer sheath of signal cables was changed and the interference noises were completely removed.

5.3 Pulse discrimination level

Channel#1, #2 and #3 could not produce neutron signals during reactor shutdown because the positions of HTICs were far from the reactor core. However the integral bias curves of system noise pulses were measured during reactor shutdown to determine the discrimination level of each pulse-counting channel. The discrimination levels were adjusted by using the integral bias curves. After reactor start-up, the integral bias curve of each channel was measured in order to confirm whether the discrimination level had been adjusted correctly. Fig. 5.2 shows the integral bias curves of channel#1, #2 and #3 which were measured at 17.28kW, 1MW and 39.2MW of reactor power, respectively. As shown in Fig. 5.2, it was verified that each discrimination level was correct. As shown in the integral bias curves of system noises in Fig. 5.2, interference noises were not observed.

5.4 Output plateau characteristics

The recommended operating voltage of HTIC is 100 V. The HTIC is able to perform the neutron flux measurement in the range from $2x10^2$ to $2x10^{10}$ n/cm^2s in such low operating voltage. The performance was verified by the test in the JRR-4. In the AVR experiment, it was very important that the output plateau characteristic of each channel was measured at the maximum reactor power in order to confirm sufficient saturation of each plateau curve. The plateau curves were measured at maximum power (42.5MW) in this experiment. Fig. 5.3 shows the measured plateau curves of channel#1, #2 and #3. Each plateau curve shows sufficient saturation at 100 V of applied voltage. It was confirmed that the neutron flux measuring system operated properly in the AVR experiment without deviating from the measurement range of each channel.

6. Results of neutron flux measurement

In the AVR experiment, the neutron flux density in the SG was continuously measured on real time from reactor start-up to 42.5MW. The neutron flux density depends not only on the reactor power but also on the steam temperature and the feed water flow rate. Fig. 6.1 shows the reactor operation data of control rod position, feed water flow rate, steam temperature etc. during the neutron flux measurement.

Fig. 6.2 shows the neutron flux densities in the SG which were measured during the stepwise reactor power increase. The neutron flux densities were obtained by using the neutron sensitivity of each HTIC when HTICs were covered with Al_2O_3 braiding sheath.

Channel#1 began to detect neutrons shortly before the AVR reached the critical state. The neutron flux density at the channel#1 position was $1.9x10^3$ n/cm^2s at 100W. The neutron flux density increased in direct proportion to the reactor power up to 3MW. After plotting on a graph, it was found that they almost formed a straight line.

The neutron flux densities at 10MW and 12.5MW were $2.2x10^8$ and $2.7x10^8$ n/cm^2s. They were rather lower than the straight line which was drawn on the basis of the data from 100W to 3MW. These deviations were due to the operation which increased the feed water flow rate rapidly from 26 t/h to 57 t/h just before the reactor power reached 10MW as in Fig. 6.1. By this operation, cold and highly dense water flowed into the SG piping, resulting in the increase of shielding ability of the SG piping for neutrons.

The neutron flux densities at 39.2MW and 42.5MW were $3.8x10^9$ and $4.2x10^9$ n/cm^2s, respectively. Those values were much higher than the straight line. The extreme increase of neutron flux was due to high temperature steam. The shielding ability of the SG piping deteriorated because the AVR power reached too high a level and the SG produced high temperature steam of over 400°C for electric power generation.

The changes of the neutron flux density at channel#2 and #3 positions showed a similar tendency to that at channel#1 position. The measured neutron flux density at channel#1 position at 42.5MW was 3.5 times higher than the value on the straight line at the same power. Those at channel#2 and #3 positions were 4.4 and 1.8 times, respectively.

As shown in Fig. 6.2, the neutron flux density of channel#1 position was measured from 100W to 42.5MW because the AVR power was increased in a stepwise operation from 100W. It was confirmed that channel#1 operated perfectly because interference noise was not observed by the oscilloscope and the measured value at 100W in Fig. 6.2 was correctly plotted on the straight line.

The indication of the channel#2 output at 1KW was 1.3cps and the neutron flux density was $2.3x10^2$ n/cm^2s. The measured value was correctly plotted on the straight line. This result proved that channel#2 operated perfectly with no interference noise from very low counts such as 1.3cps. Channel#3 also operated properly as did channel#2.

In this AVR experiment, outputs of the wide range monitors and period amplifiers were continuously recorded during start-up, power-up and high power operation of the AVR in order to confirm correct operation of the neutron flux measuring systems. As an example, Fig. 6.3 shows the result of measurement with channel#1 system. In Fig. 6.3, the output of the WRME is represented in thermal neutron flux density (n/cm^2s). The period scale is made within 15/-15 seconds for both minimum periods though the measuring range of the period amplifier is from 3 to -30 seconds. The temperature is at HTIC#1 position.

For measurement of neutron flux density in the SG, the AVR power was increased in stepwise operation mode but the reactor stopped at

3KW due to reactor scram. After this accident, the reactor was started up again and reactor power was increased up to 17.3KW in normal operation mode. Then reactor power was increased in stepwise operation from 17.3KW to 42.5MW. As shown in Fig. 6.3, it was verified that the neutron flux measuring system was able to measure neutron flux density in the range of about 8 decades with only one HTIC. Also the period indication was continuously given for neutron flux change of 8 decades.

7. Estimation of neutron flux density and temperature

The neutron flux distribution in the SG was calculated by the KFA in 1968 when the AVR was constructed. Fig. 7.1 shows the calculated neutron flux distribution in comparison with the neutron flux densities which were measured in this experiment. The solid line in the figure shows the calculated thermal neutron flux distribution at 46MW of full reactor power.

In this experiment, the neutron flux densities were measured at 42.5MW because the AVR was not operated at full power during this experiment due to restrictions from other experiment. The measured neutron flux densities are shown by circle marks in the Fig. 7.1. Table 7.1 shows the comparisons of calculated results with measured neutron flux densities at 42.5MW. The calculated results at 42.5MW were obtained by using the neutron flux distribution in Fig. 7.1 assuming that the neutron flux was directly proportional to the full reactor power of 46MW.

The measured neutron flux density at channel#1 position was 977 times higher than the calculated value. Those of channel#2 and #3 position were 471 and 19 times higher, respectively.

The accuracy of the measurements should be specified in this paper and was as follows.

The inaccuracy of the calibration for the neutron sensitivity of HTIC was between +0 and -32%. The inaccuracy of -31% was due to uncertainty of depression of neutron flux because some perturbation of neutron flux was produced during calibration of the HTIC sensitivity. The inaccuracy of -1% was due to uncertainty about the neutron shielding ability of the Al_2O_3 braiding sheath.

The indication error of the neutron flux measuring electronics with logarithmic output was between +0.03 and -0.03 decades (approximately +7% and -7%).

Therefore the total inaccuracy of measurements was between +7% and -39%.

The neutron sensitivity of HTIC is changed with temperature in the neutron field because the fission cross section of ^{235}U, which is neutron-sensitive material of HTIC, depends on neutron energy. In the AVR experiment, the outlet temperature of the cooling-gas at 42.5MW was 706° C and the temperature at channel#1 position was 443° C.

Therefore it is assumed that the neutron sensitivity of HTIC decreased due to the increase of neutron energy during high power operation of the AVR. If neutron temperature was 443°C, the neutron sensitivity of HTIC decreased about 40%. Taking account of this decrease of neutron sensitivity, the results of neutron flux measurements must be multiplied by a factor of 1.67 to obtain the real value. However, temperature distribution through the reactor core and the SG is complex and its effect upon neutron energy is very complicated. It was difficult to evaluate real neutron energy at the position of each HTIC. For the above reason, it was decided that the estimation of neutron flux densities after consideration of the neutron energy was a subject for future study. In this paper, the neutron flux densities were calculated from the neutron sensitivities of HTICs at room temperature.

Fig. 7.2 shows a comparison of the calculated temperature distribution with the measured temperatures in the SG. The solid line in the figure shows the temperature distributions at 46MW which were calculated by KFA. The circle marks show the temperatures which were measured at 42.5MW. The measured temperatures were in approximate agreement with the calculated temperature distribution.

8. Conclusion

It was demonstrated that HTIC can be used for measurement of the neutron flux in the range of 8 decades from 10^2 to 10^{10} n/cm^{2}s in an actual high temperature gas-cooled reactor. Practical techniques and experience, such as an installation method and a noise reduction method for the neutron measuring system, were obtained through this experiment. This is useful information for the case that HTICs and neutron flux measuring electronics are installed with long signal cables in a high temperature gas-cooled reactor where big electric machines such as cooling-gas blowers are operated making big electromagnetic interferences.

The neutron flux densities were measured at three positions in the SG in this experiment. It became clear that measured results were approximately 1000, 500 and 20 times higher than the results calculated in 1968, respectively. These results will be useful data for the verification of the computing code.

Calculations performed in 1989 show a better agreement with the measured results by at least a factor of ten [7].

The changing of the neutron flux density in the SG was also measured on real time during reactor power-up. The neutron flux density depended not only on reactor power but also on the SG conditions which varied with feed water flow rate, water temperature and steam temperature. The effect of such SG conditions upon the neutron flux density became clear in this experiment.

Acknowledgments

The authors are grateful to Dr. Kirch(KFA), Dr. Kaneko(JAERI) and Dr. Sanogawa(JAERI) for their supports in proceeding with the experiment at the AVR using the neutron flux measuring system with the developed HTICs. We also wish to thank Mr. Jost(AVR), Mr. Domen(AVR) and other staff members at the AVR for their help in carrying out this experiment.

References

[1] GOODINGS,A., HAGGER,H., PHILLIPS,R.D., "Reactor control neutron detectors for operation at high temperature", Inst. Elect. Eng., Publication No.47(1968)37.

[2] MOBBS,D.J., Neutron detectors for reactor control, J. Inst. Nucl. Eng. 181(1977)16.

[3] Neutron Gas Filled Detectors, Catalogue-R.T.C. La Radiotechnique-Compelec, Ref. 4270-05-1977(1977).

[4] AOCHI,T., et al., First conceptual design of the experimental multi-purpose high-temperature gas-cooled reactor, JAERI-M6845(1977).

[5] WAKAYAMA,N., GOTOH,H., TOMODA,T., High temperature neutron detector development, JAERI-M5955(1975)131.

[6] WAKAYAMA,N., YAMAGISHI,H., TOMODA,T., KAWASHIMA,K., "Development of fission chambers for high-temperature reactors", IAEA SM-226/32, Nucl. Power Plant Cont. & Inst.(1978).

[7] JANKE, LEE, QUADE, AVR-Test-Program, Final Report, No 70-04678.7 (Nov 89).

List of figures, tables and photographs

Table 1.1 Technical data of AVR
Figure 1.1 Construction of the AVR
Table 2.1 Specifications of Wide Range High Temperature In-core Fission Counter-chamber (HTIC)
Figure 2.1 Structure of Wide Range High Temperature In-core Fission Counter-chamber (HTIC)
Figure 2.2 Schematic block diagram of Wide Range Neutron Measuring Electronics (WRME)
Figure 2.3 Front panel view of Wide Range Neutron Measuring Electronics (WRME)
Figure 2.4 Output linearities of Neutron Flux Measuring System (NFMS) measured in JRR-4
Figure 3.1 Dimensions of graphite pile with neutron sources for neutron sensitivity calibration of HTIC
Figure 3.2 Dimensions of HTICs for AVR experiment
Table 3.1 Results of examination of HTIC#1(FA-1-31)
Table 3.2 Results of examination of HTIC#1(FA-1-32)
Table 3.3 Results of examination of HTIC#1(FA-1-33)
Figure 4.1 Composition of HTICs assembled for AVR experiment
Figure 4.2 Dimensions of assembly composed of HTICs and thermocouples
Figure 4.3 Complete construction of penetration rig for installation of HTIC assembly into AVR
Figure 4.4 Side view of penetration flange
Figure 4.5 Upper view of penetration flange
Figure 4.6 Structure of penetration for signal cable of HTIC and thermocouple
Figure 4.7 Positions of HTICs, TCs, cabling and electronics installed in AVR
Figure 4.8 Detailed positions of HTICs and TCs installed in AVR
Photo. 4.1 Complete views of assembly composed of three HTICs, seven thermocouples and one penetration flange
Photo. 4.2 Top part view of assembly with HTIC#1, TC#5 and TC#6
Photo. 4.3 Middle part view of assembly with HTIC#2, TC#7 and TC#8
Photo. 4.4 Middle part view of assembly with HTIC#3, TC#9 and TC#10
Photo. 4.5 Upper part view of assembly with penetration flange
Photo. 4.6 Side view of penetration flange for connections of signal cables
Photo. 4.7 Upper view of penetration flange for connections of signal cables
Photo. 4.8 Views of carrying HTIC assembly from KFA to AVR
Photo. 4.9 Wideband preamplifier box installed on the outside wall of reactor containment
Photo. 4.10 Wide Range Neutron Measuring Electronics mounted on racks in the instruments room of AVR

Figure 5.1 Block diagram of Neutron Flux Measuring System for AVR experiment
Figure 5.2 Integral bias curves of HTICs measured in AVR
Figure 5.3 Plateau curves of THICs measured at 42.5MW in AVR
Figure 6.1 Operation data of AVR during reactor power-up
Figure 6.2 Neutron flux in the steam generator measured at various reactor powers of AVR
Figure 6.3 Neutron flux and reactor period measured on real time during reactor power-up
Figure 7.1 Comparison of calculated neutron flux distributions with experimental results at 42.5MW
Table 7.1 Comparison of measured neutron flux with calculated results
Figure 7.2 Comparison of calculated temperature distribution with measured temperature

Table 1.1 Technical data of AVR, Reference : Pamphlet of "Der Kugelhaufenreaktor der Arbeitsgemeinschaft Versuchsreaktor (AVR)"

Items	Specifications
Reactor	
full thermal power	46MW
diameter of core	3000mm
average height of core	2800mm
number of fuel elements	92000pieces
helium gas pressure	10.8bar
inlet temp. of helium gas	275℃
outlet temp. of helium gas	950℃
Fuel	
diameter of fuel ball	60mm
fuel material	U, Th
quantity of uranium-235	1g
enrichment	10, 16.7, 93%
quantity of thorium	0, 5, 10g
Steam generator	
numbers	4 system/section
type	forced circulation
inlet temp. of feed water	115℃
outlet temp. of superheated steam	505℃
flow rate of steam	56t/h
Pressure vessel	
diameter of inner vessel	5780mm
height of inner vessel	24910mm
diameter of outer vessel	7600mm
height of outer vessel	26045mm
Generator	
full power	15MW

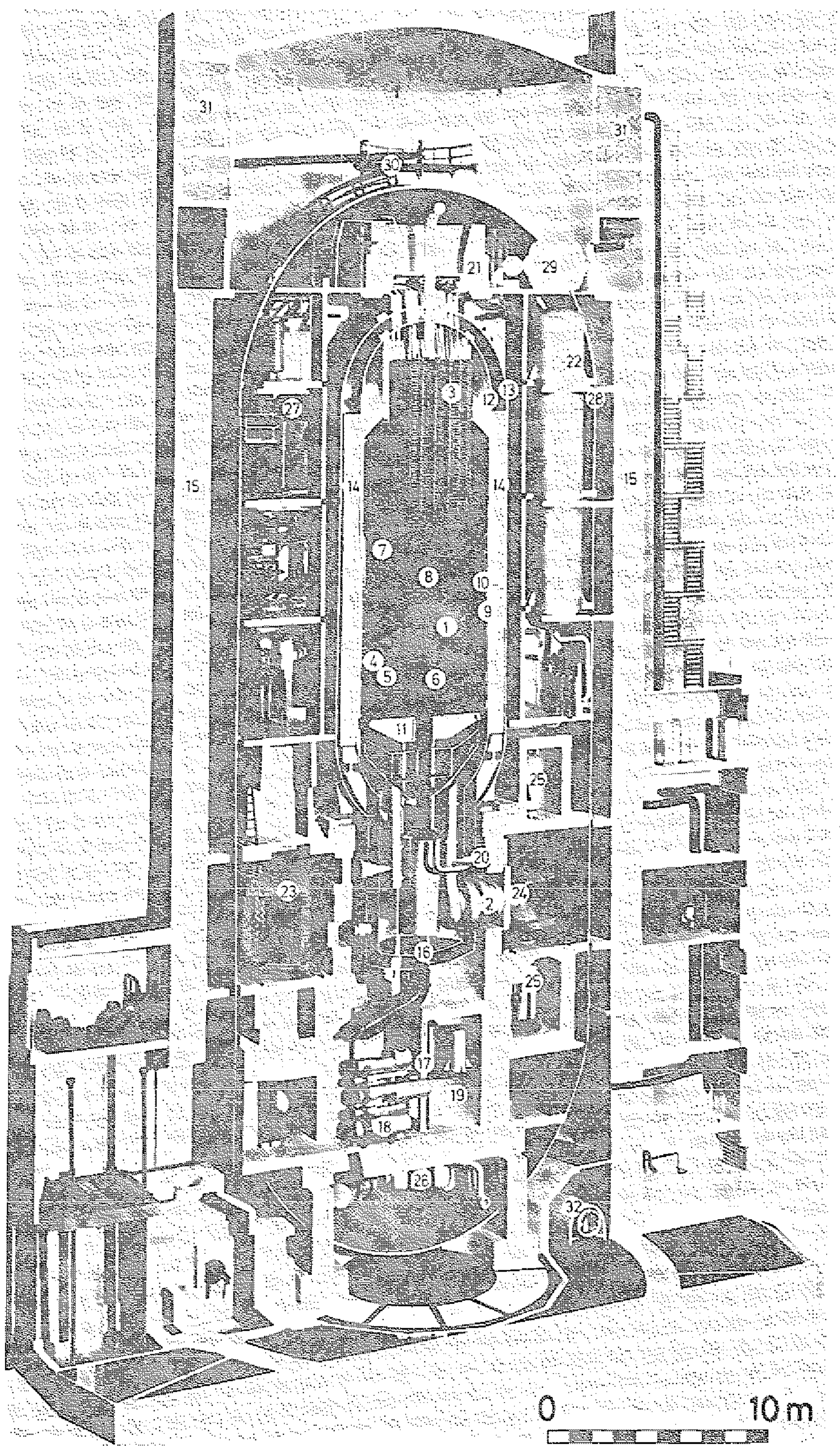

1 Reactor core
2 Cooling gas blower
3 Steam generator
4 Carbon construction
5 Side reflector
6 Bottom reflector
7 Top reflector
8 Graphite column for control rod
9 Thermal shield
10 Fuel charge pipe
11 Star-shaped support
12 Inner vessel
13 Outer vessel
14 Biological shield 1
15 Biological shield 2
16 Fuel discharge pipe
17 Control rod
18 Failed fuel selector
19 Fuel circulator room
20 Main gas valve
21 Steam collector
22 Mixture cooler
23 Installation unit
24 Cover lift
25 Gas refining unit
26 Water drain tank
27 Air circulating unit
28 Containment
29 Personal air lock
30 Sprinkler
31 Upper water tank
32 Ring channel

Fig. 1.1 Construction of the AVR, Reference : Pamphlet of "Der Kugelhaufenreaktor der Arbeitsgemeinschaft Versuchsreaktor (AVR)"

Table 2.1 Specifications of Wide Range High Temperature In-core Fission Counter-chamber (HTIC)

Items	Specifications
Size	
outside diameter	10mm
sensitive length	80mm
gap of electrodes	1.0mm
diameter of MI-cable	ϕ 5mm
Material	
vessel(cathode)	Hastelloy-X
anode	Hastelloy-X
insulator	Al_2O_3
neutron sensitive material	U_3O_8 (E:93%)
ionized gas	$Xe+5\%N_2+1\%He$
conductor of MI-cable	Cu/Inconel
sheath of MI-cable	Inconel 600
insulator of MI-cable	MgO
Operating performance	
thermal neutron sensitivity	0.01cps/nv
operating voltage	100V
current pulse height	1.6 μA
charge pulse height	0.8×10^{-13}c
electron collection time	100ns
Maximum rating	
operating temperature	800℃
thermal neutron flux	2.6×10^{10}nv

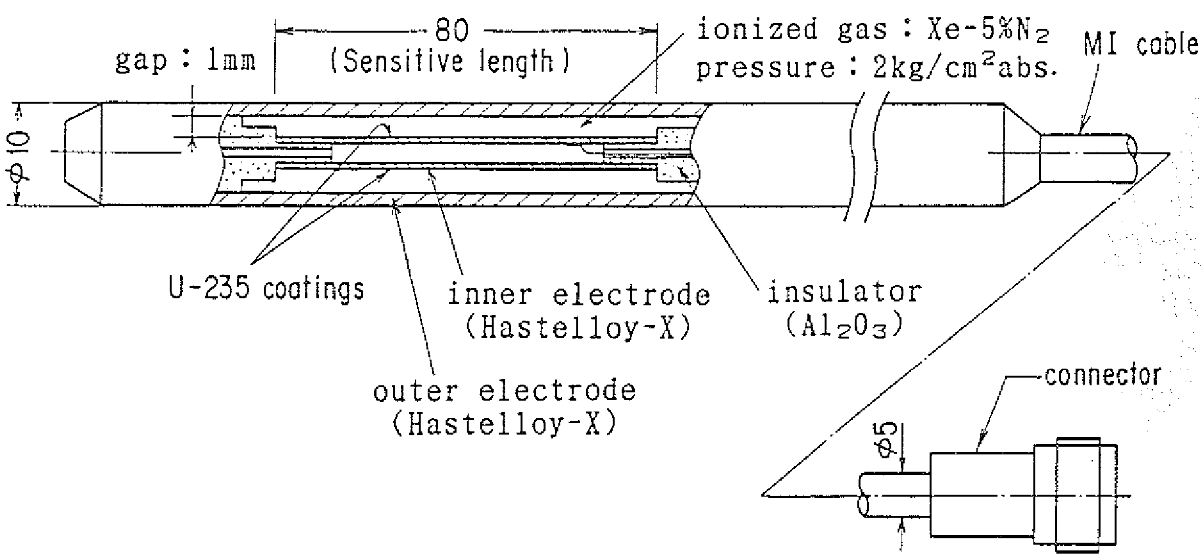

Fig. 2.1 Structure of Wide Range High Temperature In-core Fission Counter-chamber (HTIC)

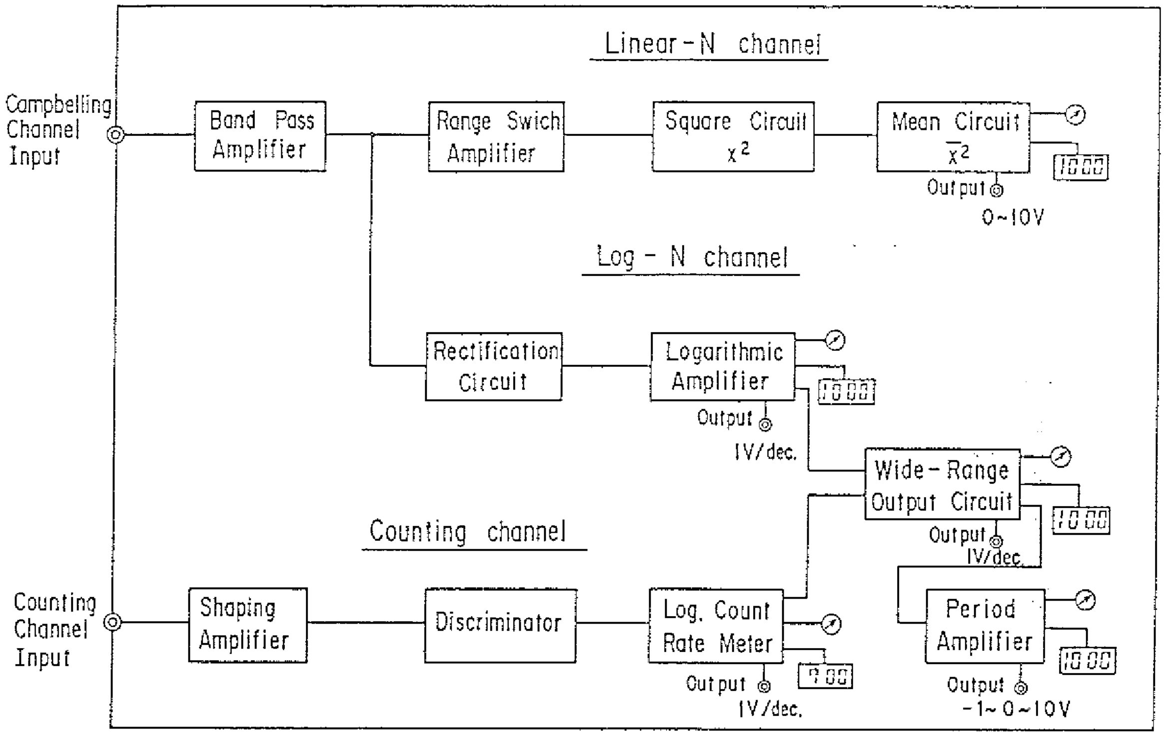

Fig. 2.2 Schematic block diagram of Wide Range Neutron Measuring Electronics (WRME)

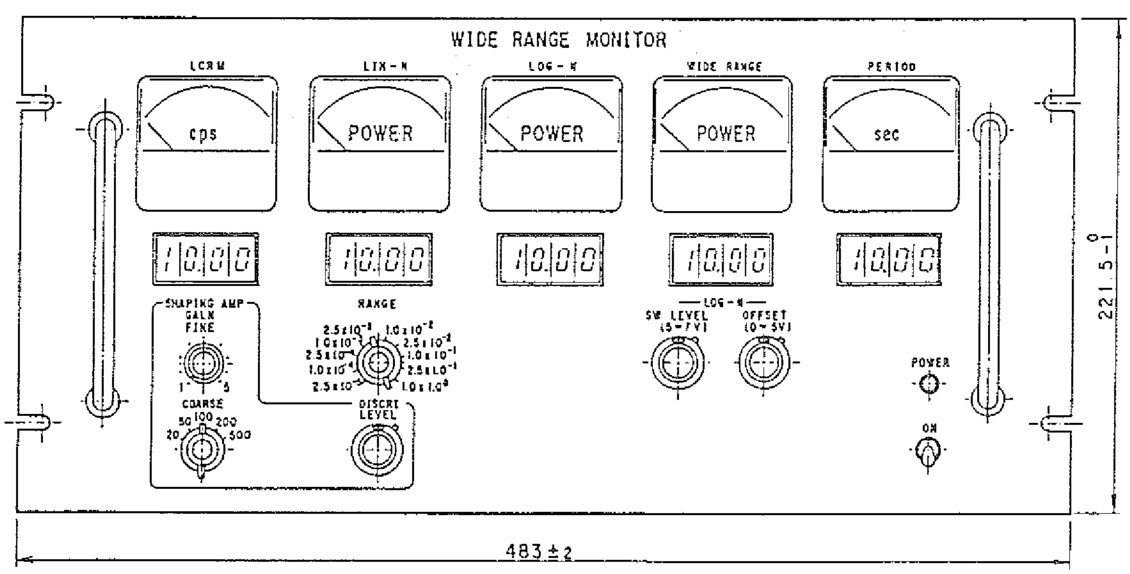

Fig. 2.3 Front panel view of Wide Range Neutron Measuring Electronics (WRME)

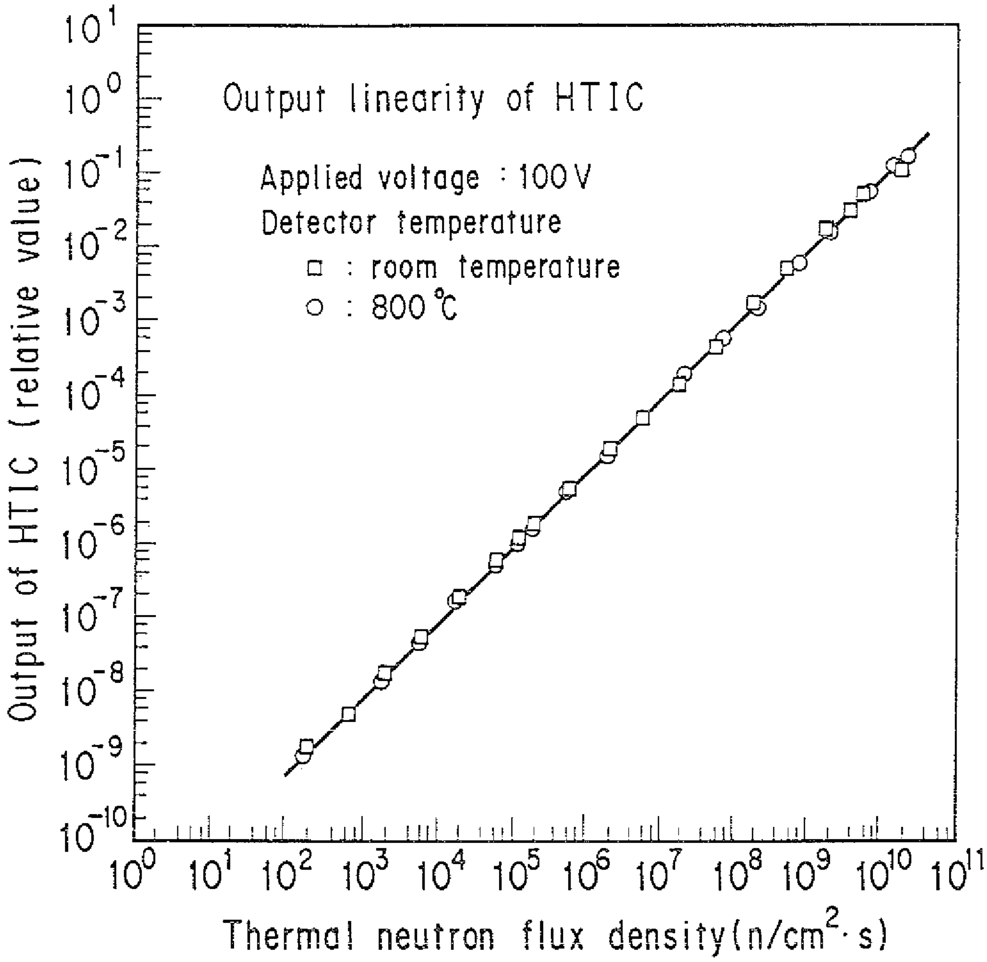

Fig. 2.4 Output linearities of Neutron Flux Measuring System (NFMS) measured in JRR-4

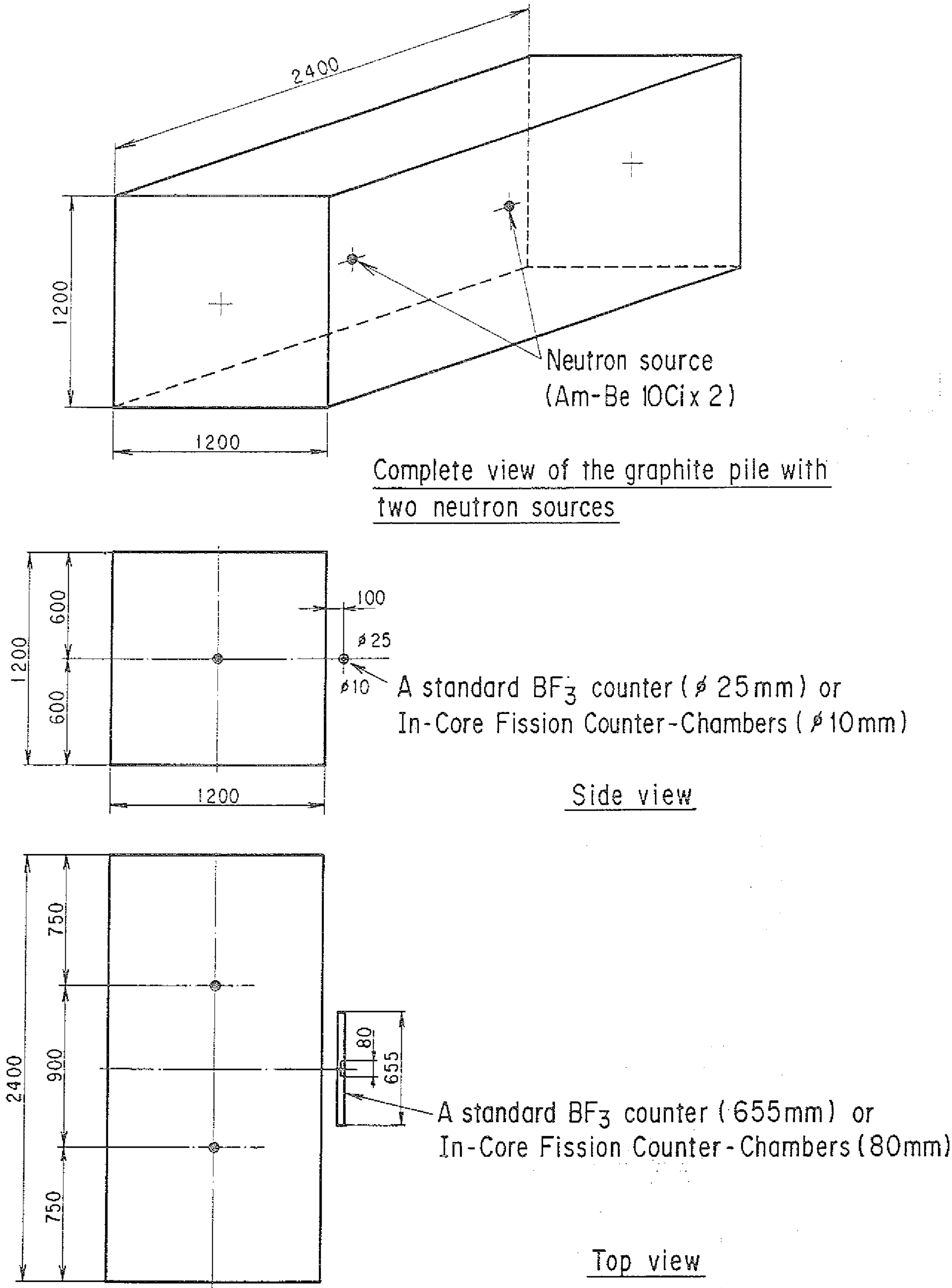

Fig. 3.1 Dimensions of graphite pile with neutron sources for neutron sensitivity calibration of HTIC

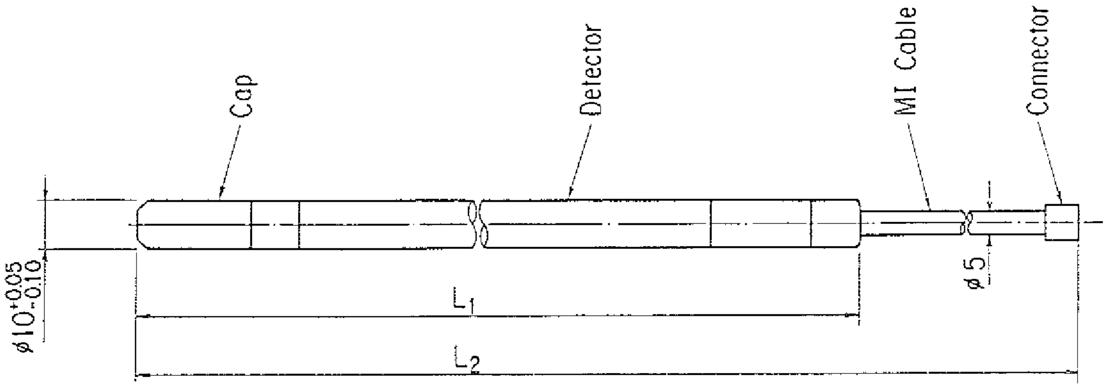

	L_1	L_2	Model
G01	413	5250	FA-1-31
G02	413	6750	FA-1-32
G03	1013	8550	FA-1-33

Fig. 3.2 Dimensions of HTICs for AVR experiment

Table 3.1 Results of examination of HTIC#1(FA-1-31)

TEST PERFORMANCE SHEET

Item	High Temperature Incore Fission Counter				
Tube Type No.	ND−8664				
Serial No.	FA−1−31				
No.	Headings		Standards	Results	Judgment
1.	Size	(1) Detector Dia.	$\phi 10\ ^{+0.05}_{-0.10}$ mm	φ9.90 ~ φ9.98 mm	OK
		(2) Detector Length	413 ±10mm	414 mm	OK
		(3) MI Cable Length	5250 ±100mm	5297 mm	OK
		(4) MI Cable Dia	φ 5 ±0.05mm	φ5.00 mm	OK
2.	Structure	(1) Gas Leakage	≤0.001 Pa cm³/sec	≤0.0001 Pa cm³/sec	OK
		(2) X-ray Photo	With no harmful defects	no defects	OK
3.	Operating Spec	(1) Operating Temp	850°C	850°C	OK
		(2) Supply Voltage	≥130V	150V	OK
		(3) Thermal Neutron Sens.	≥0.003 cps/nv	0.0068 cps/nv	OK
		(4) Peak Charge	$\geq 3.5\times10^{-14}$ C	R.T. 8.1×10^{-14} C	OK
				850℃ 3.9×10^{-14} C	OK
		(5) Resistance Det.+Cable	≥1×10[illegible] Ω	R.T. 1.2×10^{10} Ω	OK
		Det.+Cable	$\geq 5\times10^{5}$ Ω	850℃ 1.0×10^{6} Ω	OK
		(6) PBH Voltage	≥130V	150 V	OK

perfomed by M. Tamura
Date. '88 6/7~10
approved by T Shinozaki
Date. 13-6-'88

Table 3.2 Results of examination of HTIC#1(FA-1-32)

TEST PERFORMANCE SHEET

Item	High Temperature Incore Fission Counter
Tube Type No.	ND−8664
Serial No.	FA−1−32

No.	Headings	Standards	Results	Judgment
1.	Size (1) Detector Dia.	$\phi 10^{+0.05}_{-0.10}$ mm	φ9.90～φ9.98 mm	ok
	(2) Detector Length	413 ±10mm	414 mm	ok
	(3) MI Cable Length	6750 ±100mm	6810 mm	ok
	(4) MI Cable Dia	φ 5 ±0.05mm	φ5.00 mm	ok
2.	Structure (1) Gas Leakage	≤0.001 Pa cm³/sec	≤0.0001 Pa cm³/sec	OK
	(2) X-ray Photo	With no harmful defects	no defects	ok
3.	Operating Spec (1) Operating Temp	850°C	850°C	ok
	(2) Supply Voltage	≥130V	150V	ok
	(3) Thermal Neutron Sens.	≥0.003 cps/nv	0.0070 cps/nv	ok
	(4) Peak Charge	≥3.5×10⁻¹⁴C	R.T. 8.6×10⁻¹⁴ C	ok
			850℃ 8.6×10⁻¹⁴ C	ok
	(5) Resistance Det.+Cable	≥1×10⁹ Ω	R.T. 3.0×10¹² Ω	ok
	Det.+Cable	≥5×10⁵ Ω	850℃ 1.2×10⁶ Ω	ok
	(6) PBN Voltage	≥130V	150V	ok

perfomed by	M. Tamura
Date.	'88 6/7～10
approved by	T. Shinsei
Date.	13−6−'88

Table 3.3 Results of examination of HTIC#1(FA-1-33)

TEST PERFORMANCE SHEET

Item	High Temperature Incore Fission Counter
Tube Type No.	ND−8664
Serial No.	FA−1−33

No.	Headings	Standards	Results	Judgment
1.	Size (1) Detector Dia	$\phi 10^{+0.05}_{-0.10}$ mm	φ9.91～φ9.98 mm	ok
	(2) Detector Length	1013 ±10mm	1014 mm	ok
	(3) MI Cable Length	8550 ±100mm	8598 mm	ok
	(4) MI Cable Dia	φ 5 ±0.05mm	φ5.00 mm	ok
2.	Structure (1) Gas Leakage	≤0.001 Pa cm³/sec	0.0001 Pa cm³/sec	ok
	(2) X-ray Photo	With no harmful defects	no defect	ok
3.	Operating Spec (1) Operating Temp	850°C	850°C	ok
	(2) Supply Voltage	≥130V	160V	ok
	(3) Thermal Neutron Sens.	≥0.003 cps/nv	0.0068 cps/nv	ok
	(4) Peak Charge	≥3.5×10⁻¹⁴C	R.T. 7.5×10⁻¹⁴ C	ok
			850℃ 7.2×10⁻¹⁴ C	ok
	(5) Resistance Det.+Cable	≥1×10⁹ Ω	R.T. 1.0×10¹² Ω	ok
	Det.+Cable	≥5×10⁵ Ω	850℃ 1.5×10⁶ Ω	ok
	(6) PBN Voltage	≥130V	160V	ok

perfomed by	M. Tamura
Date.	'88 6/7～10
approved by	T. Shinsei
Date.	13−6−'88

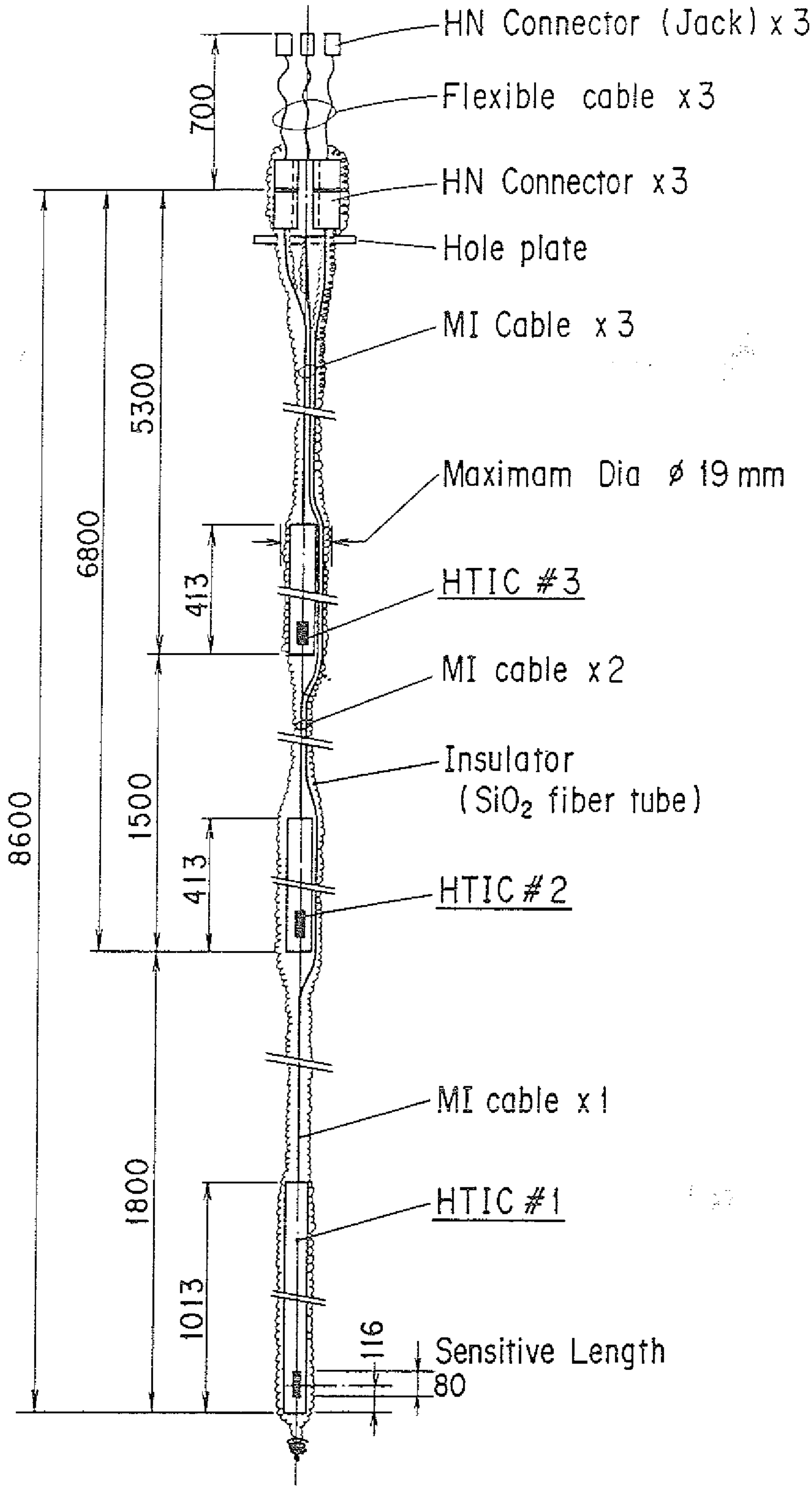

Fig. 4.1 Composition of HTICs assembled for AVR experiment

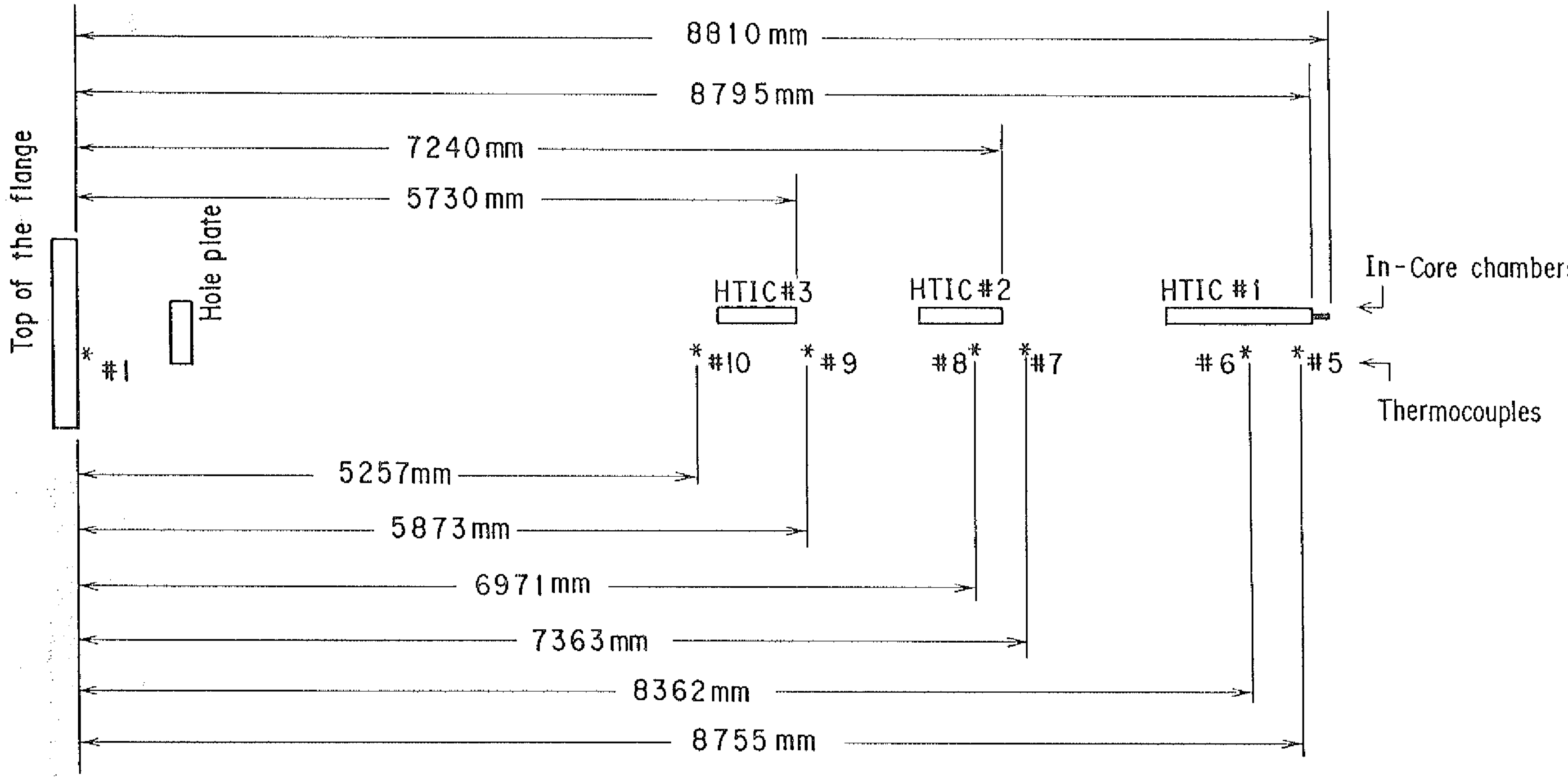

Fig. 4.2 Dimensions of assembly composed of HTICs and thermocouples

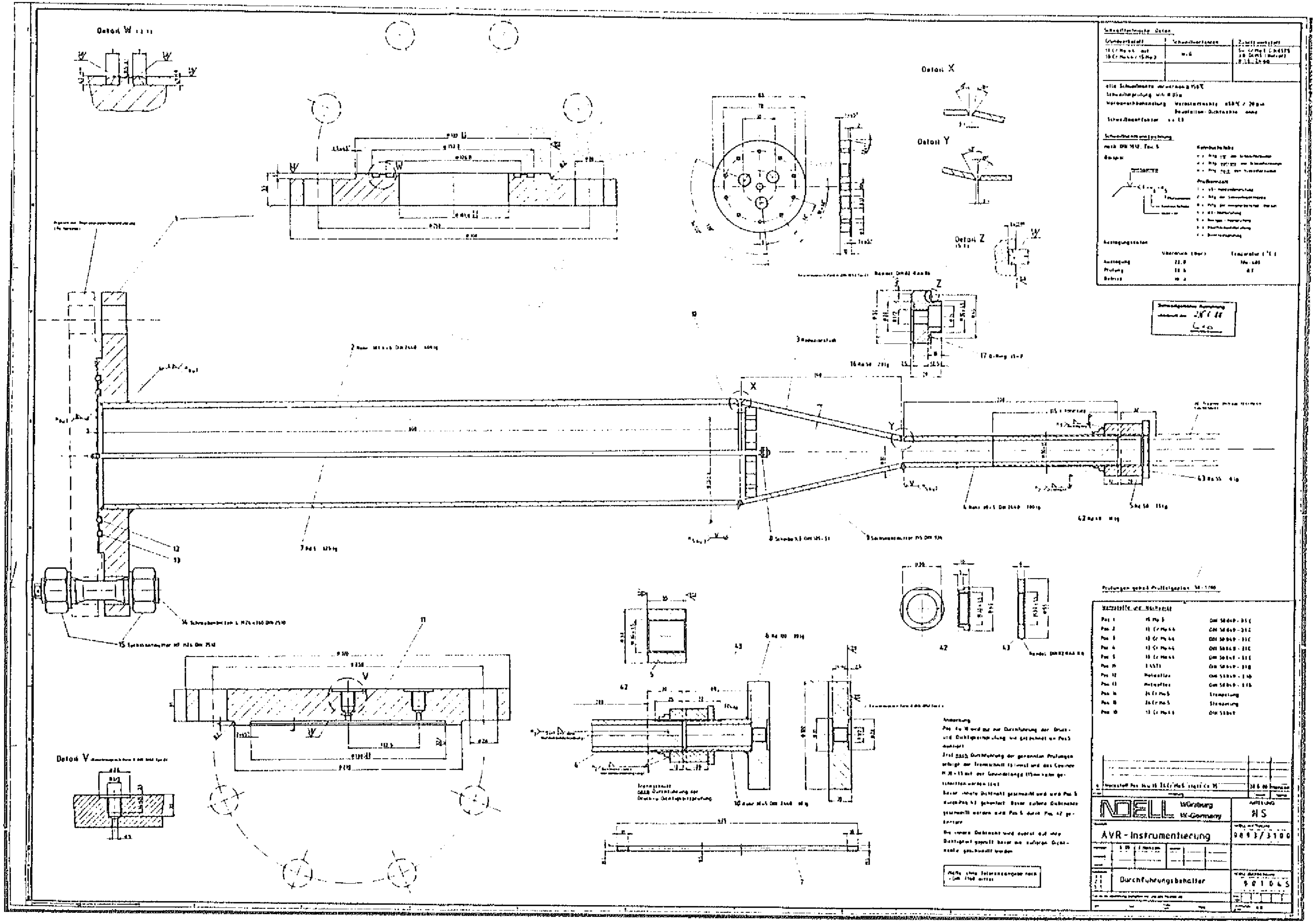

Fig. 4.3 Complete construction of penetration rig for installation of HTIC assembly into AVR (presented by KFA GmbH)

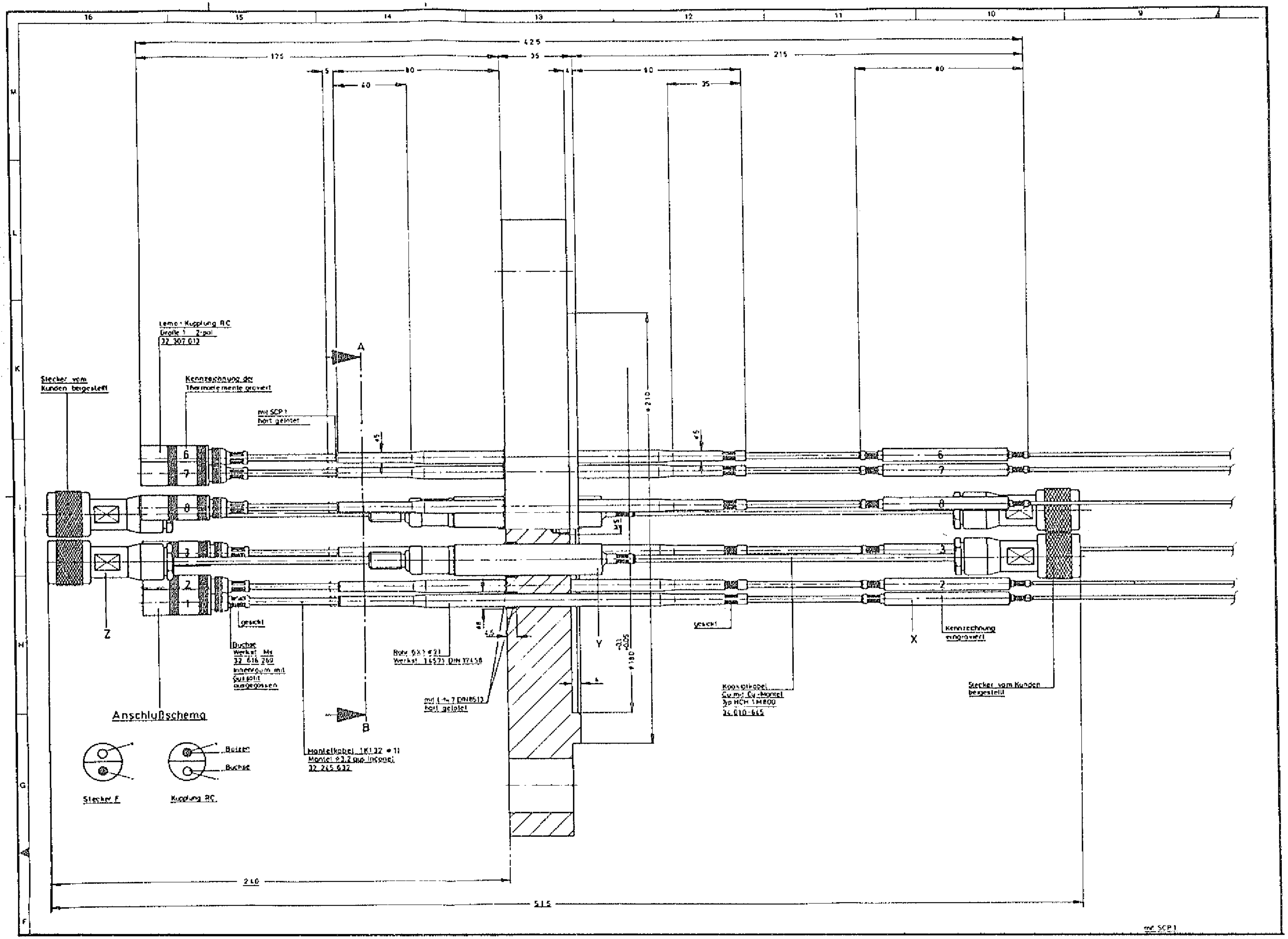

Fig. 4.4 Side view of penetration flange
(presented by KFA GmbH)

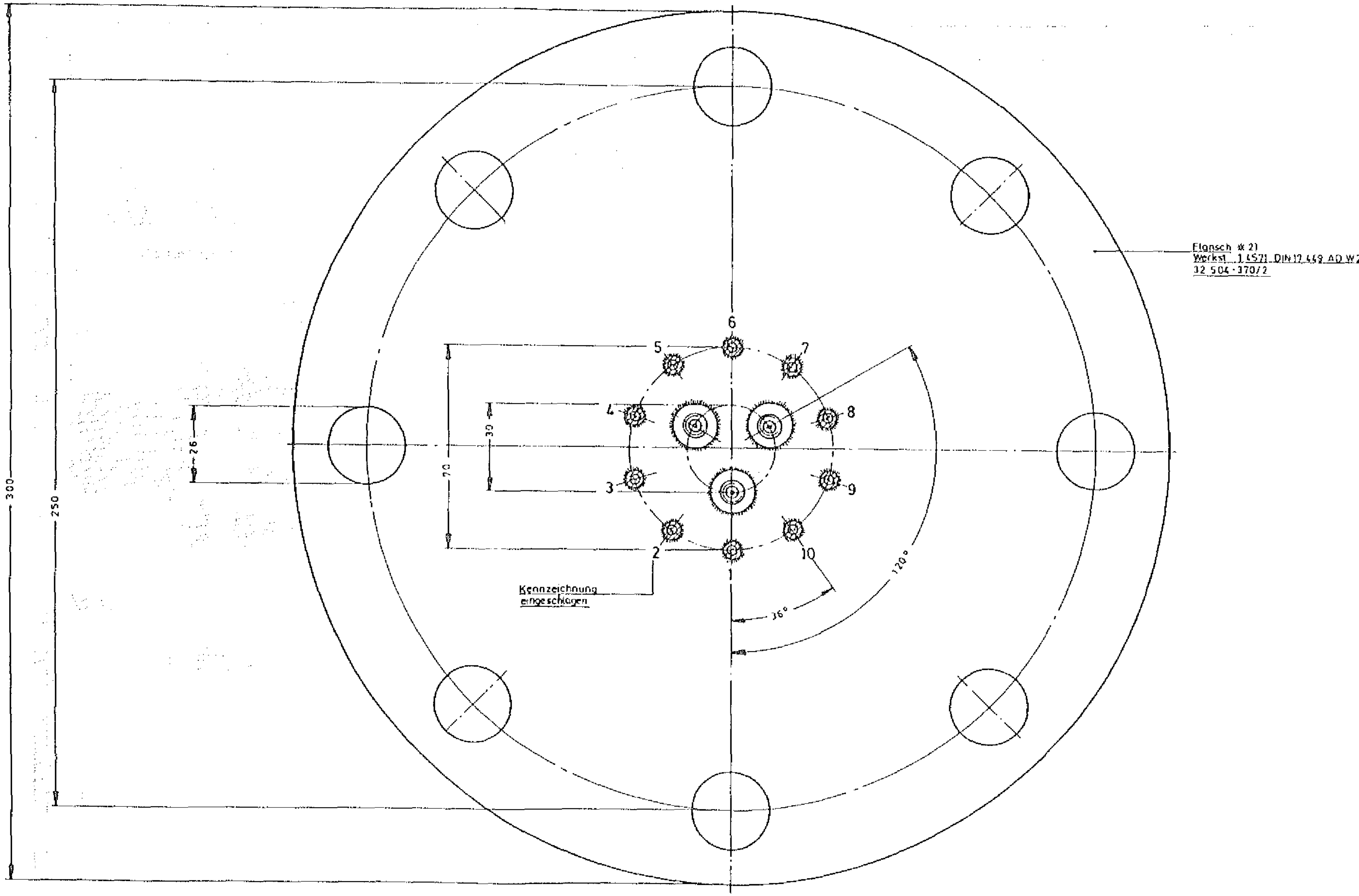

Fig. 4.5 Upper view of penetration flange
(presented by KFA GmbH)

Einzelheit X M2:1

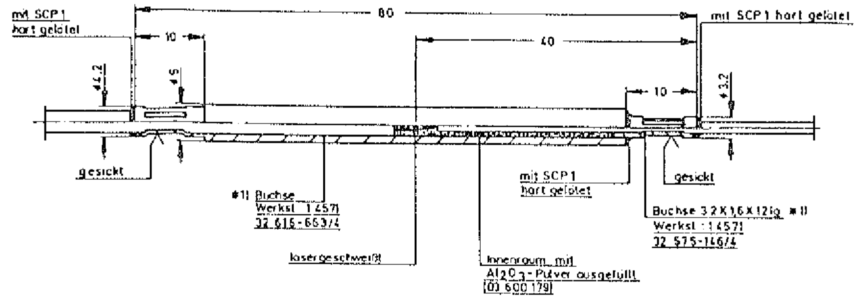

Einzelheit Y M2:1

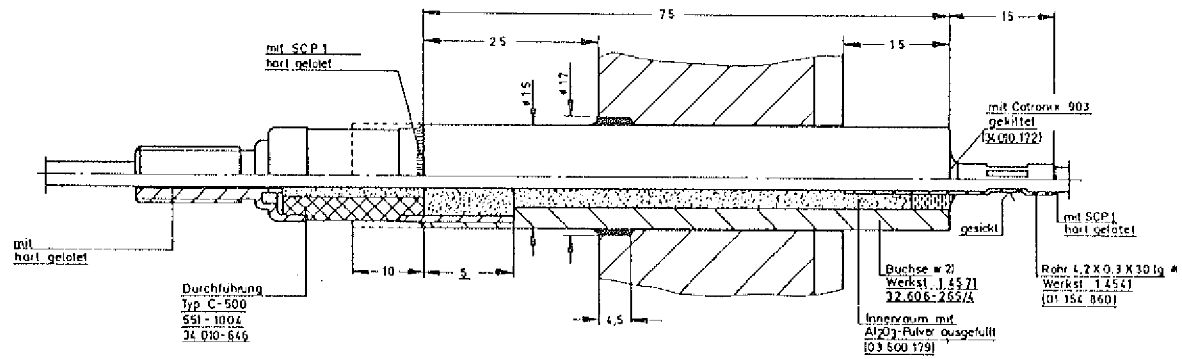

Einzelheit Z M2:1

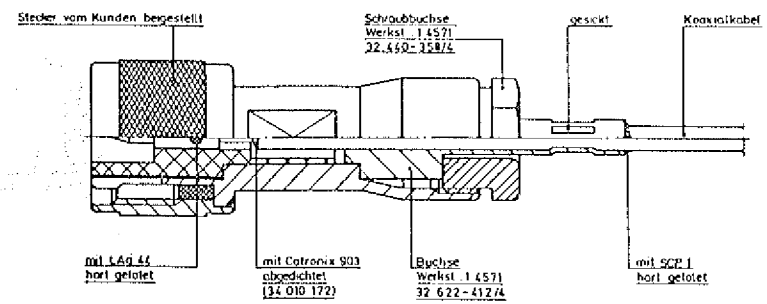

Fig. 4.6 Structure of penetration for signal cable of HTIC and thermocouple (presented by KFA)

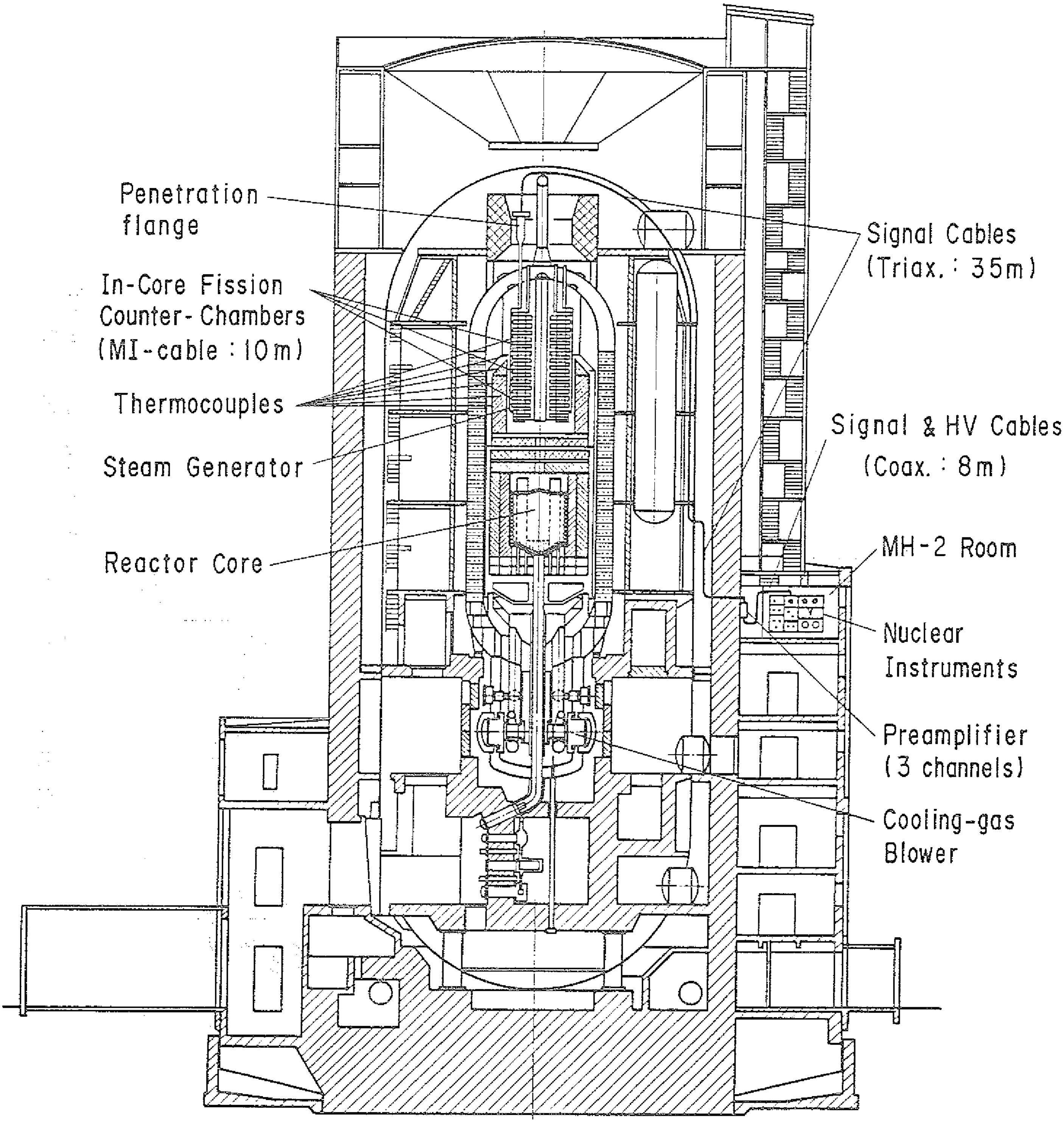

Fig. 4.7 Positions of HTICs, TCs, cabling and electronics installed in AVR (presented by KFA GmbH)

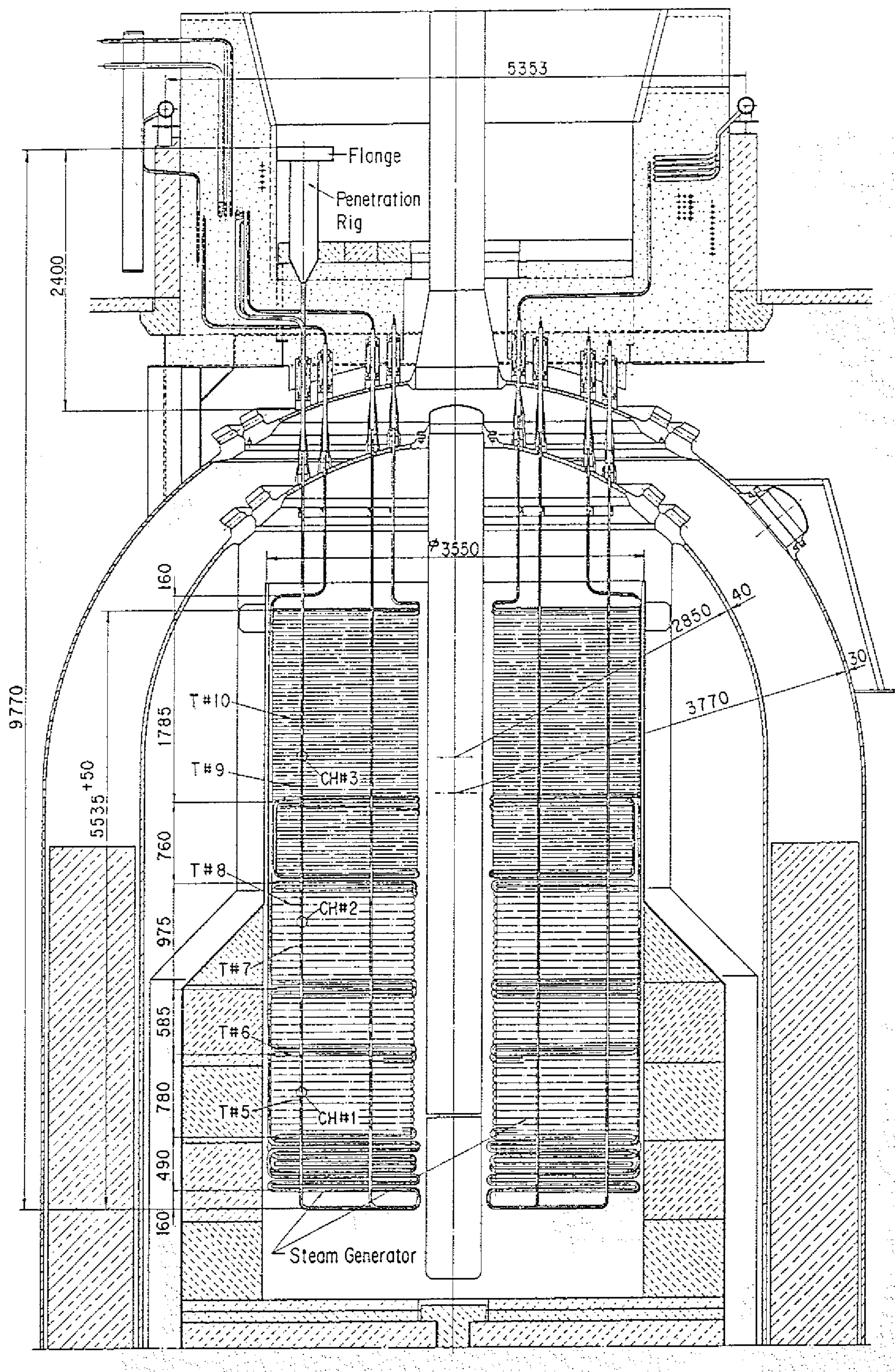

Fig. 4.8 Detailed positions of HTICs and TCs installed in AVR (presented by AVR GmbH)

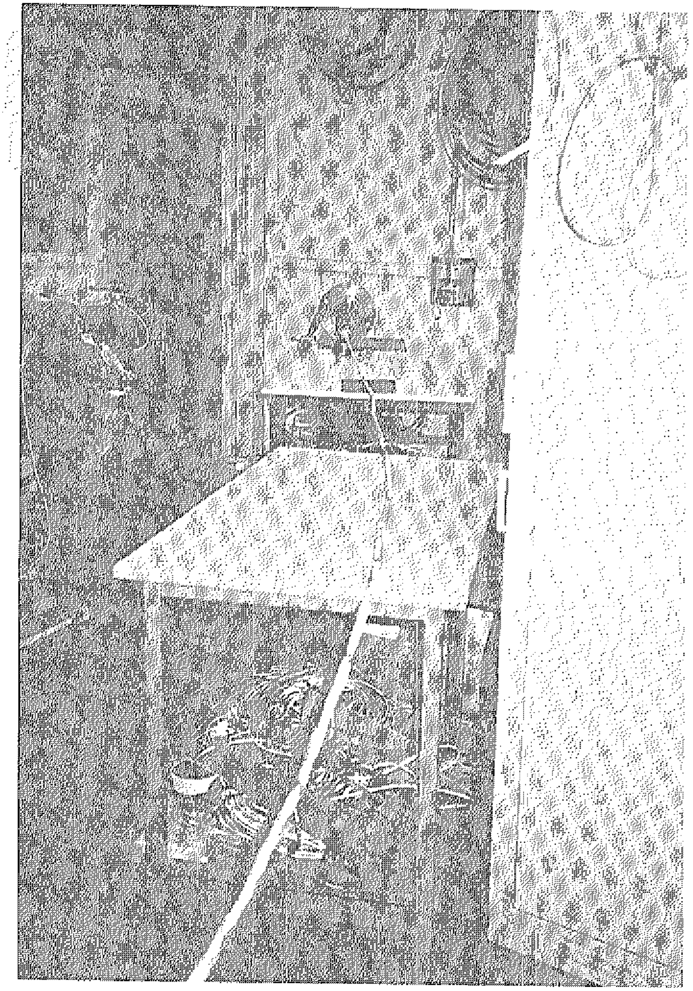

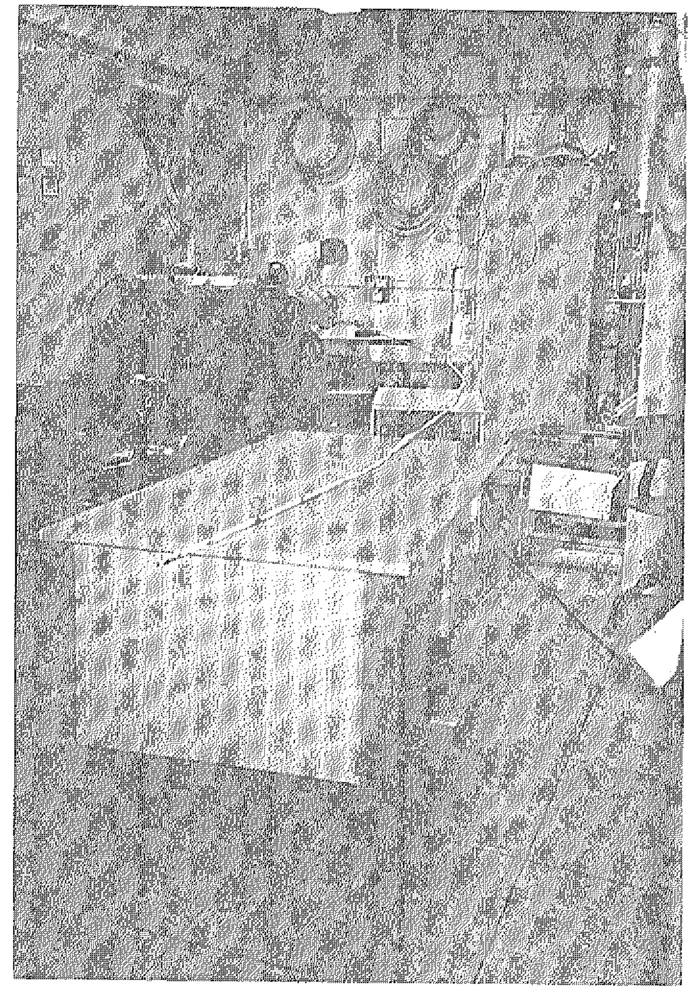

Photo. 4.1 Complete views of assembly composed of three HTICs, seven thermocouples and one penetration flange

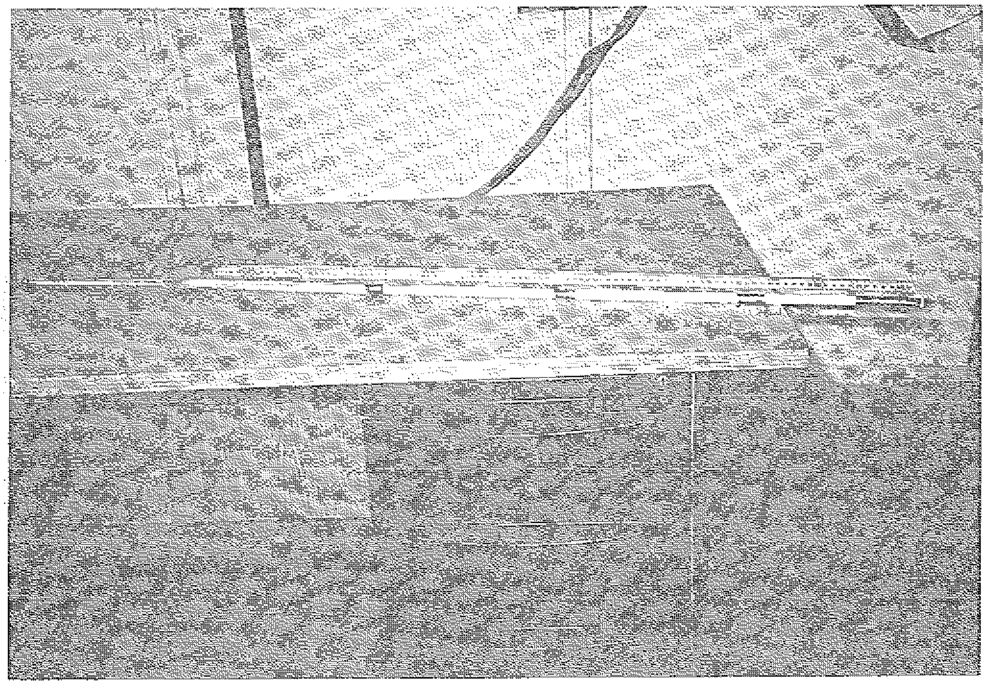

Photo. 4.2 Top part view of assembly with
HTIC#1, TC#5 and TC#6

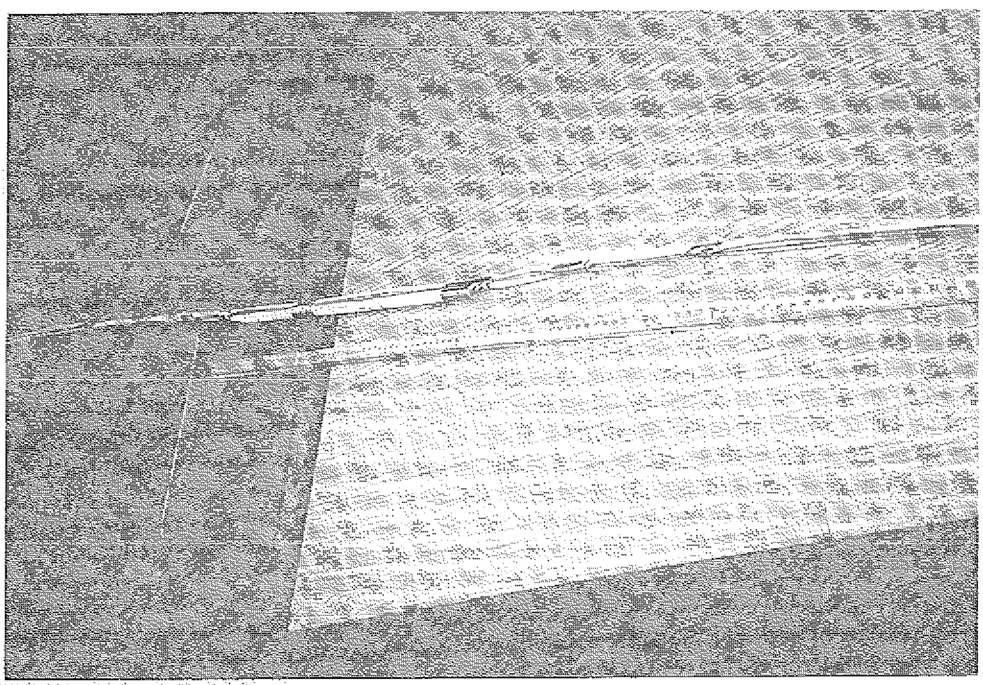

Photo. 4.3 Middle part view of assembly
with HTIC#2, TC#7 and TC#8

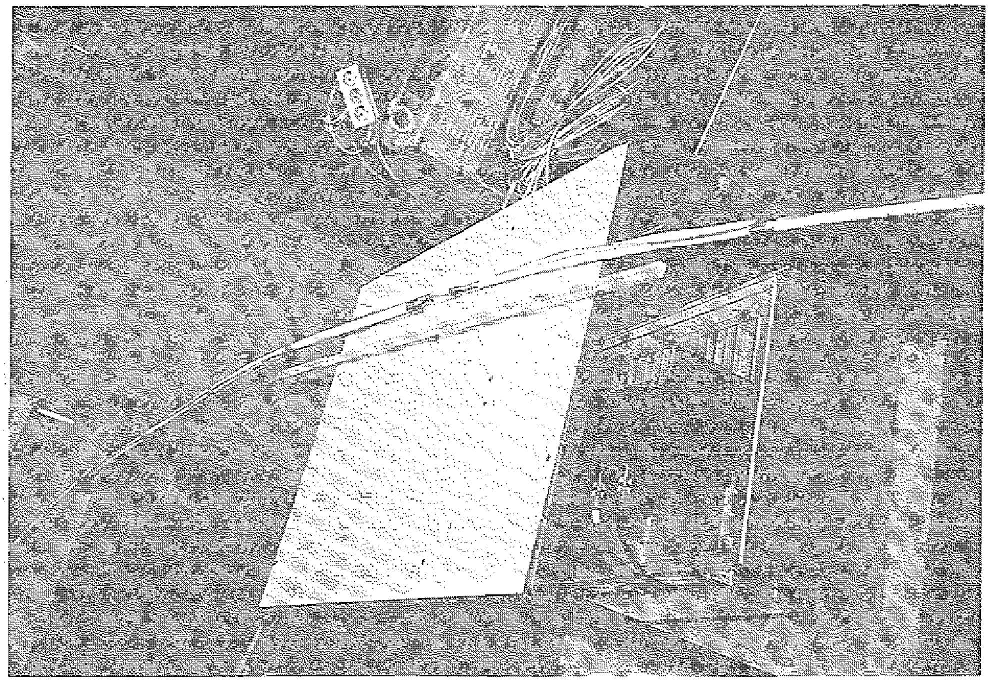

Photo. 4.4 Middle part view of assembly
with HTIC#3, TC#9 and TC#10

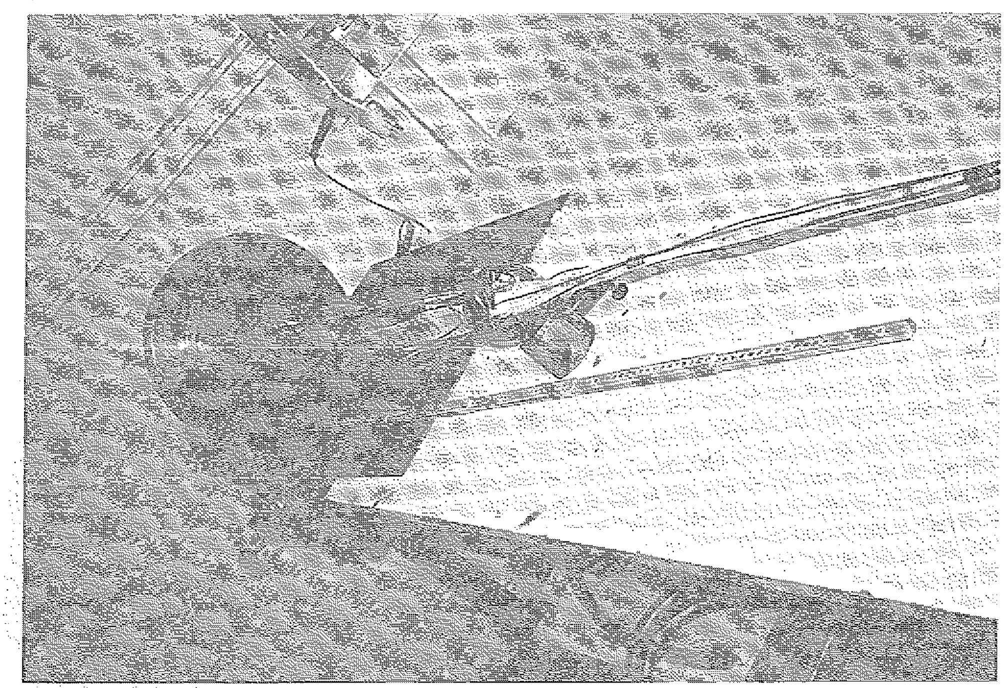

Photo. 4.5 Upper part view of assembly
with penetration flange

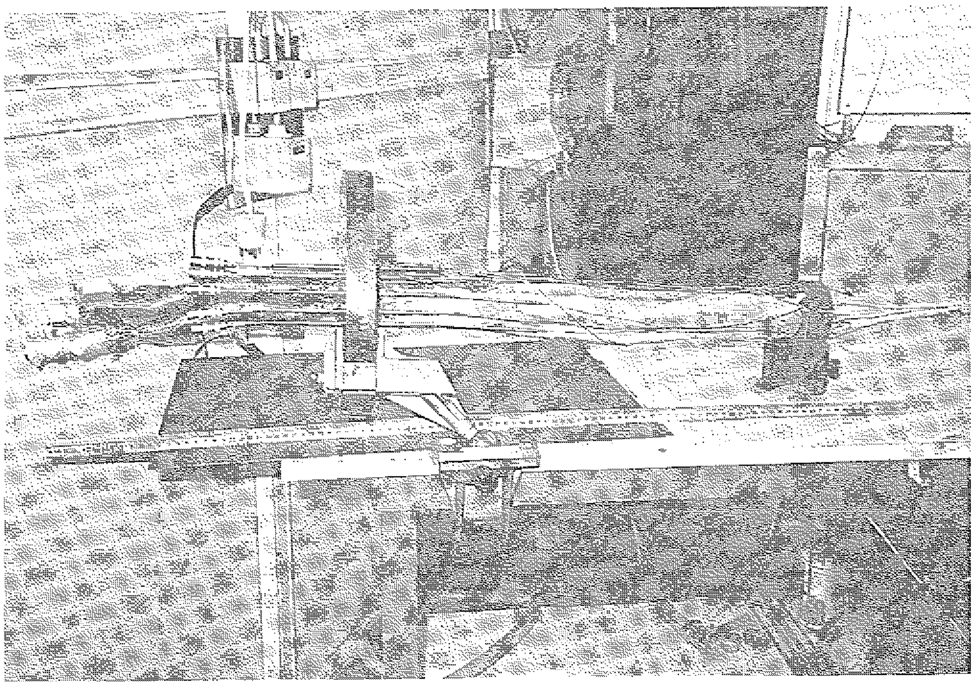

Photo. 4.6 Side view of penetration flange for connections of signal cables

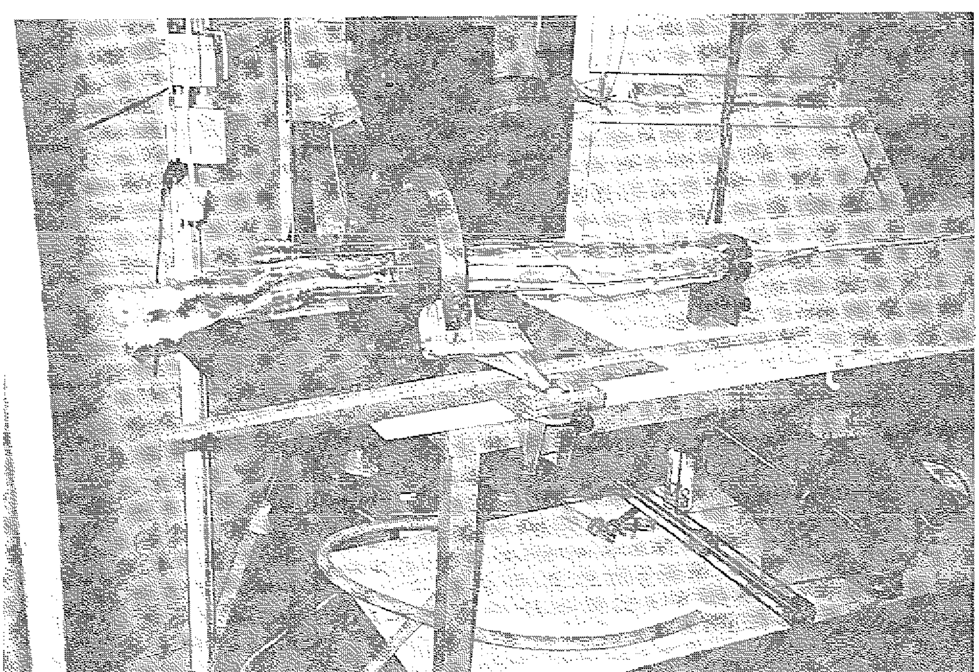

Photo. 4.7 Upper view of penetration flange for connections of signal cables

Photo. 4.8 Views of carrying HTIC assembly
from KFA to AVR

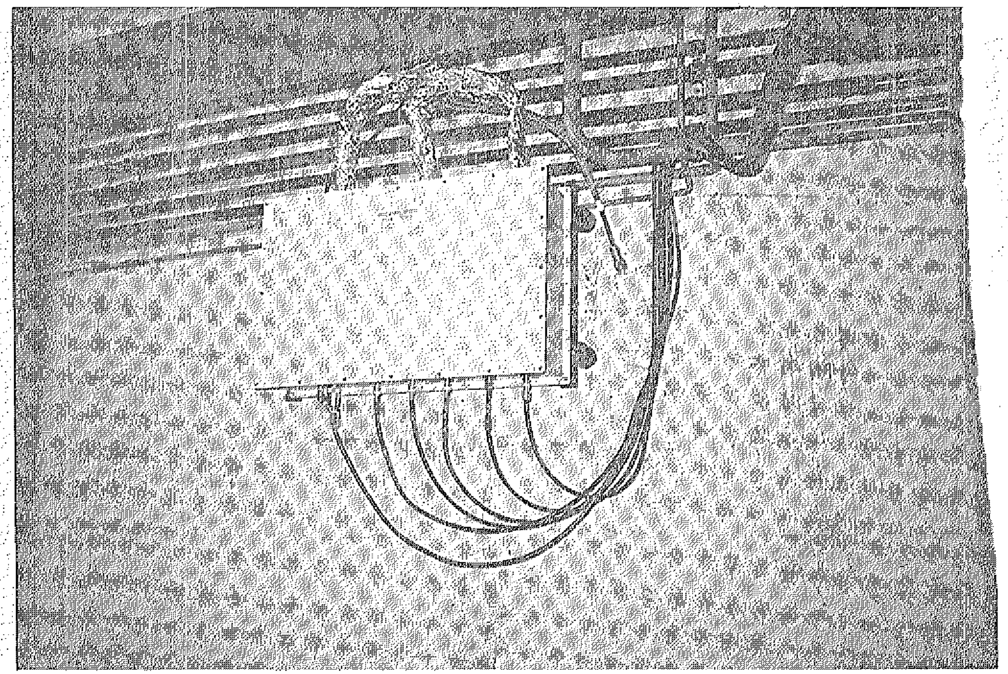

Photo. 4.9 Wideband preamplifier box installed on the outside wall of reactor containment

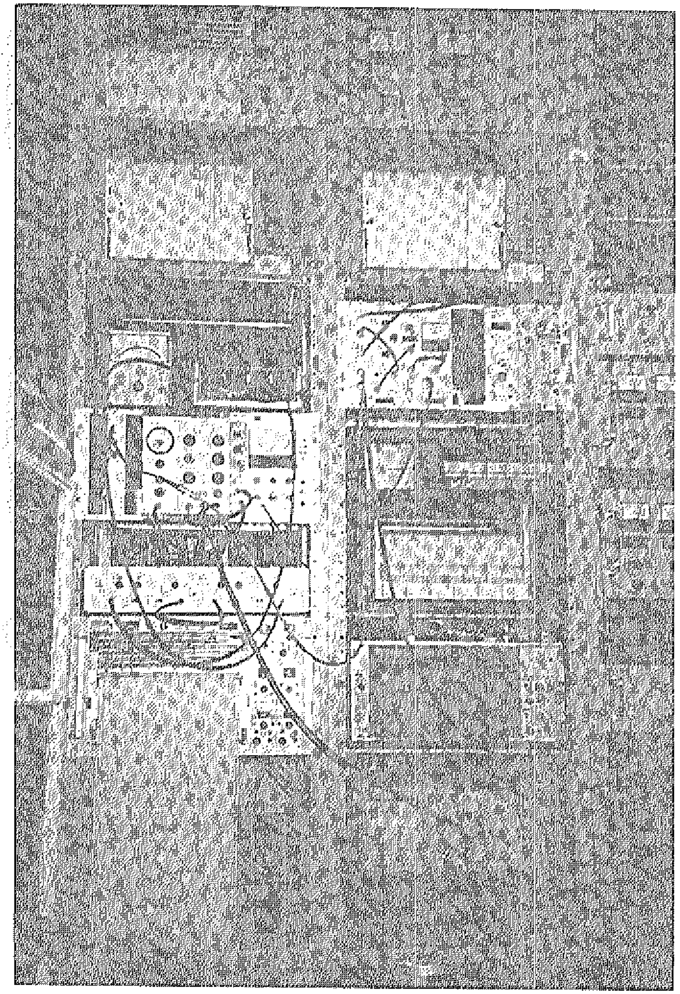

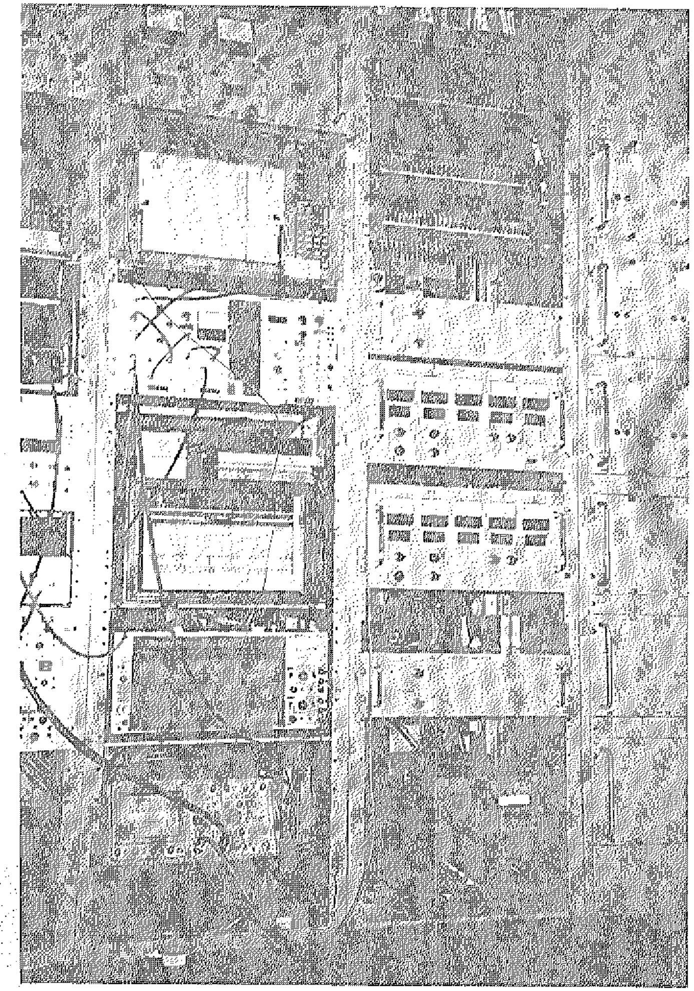

Photo. 4.10 Wide Range Neutron Measuring Electronics mounted on racks in the instruments room of AVR

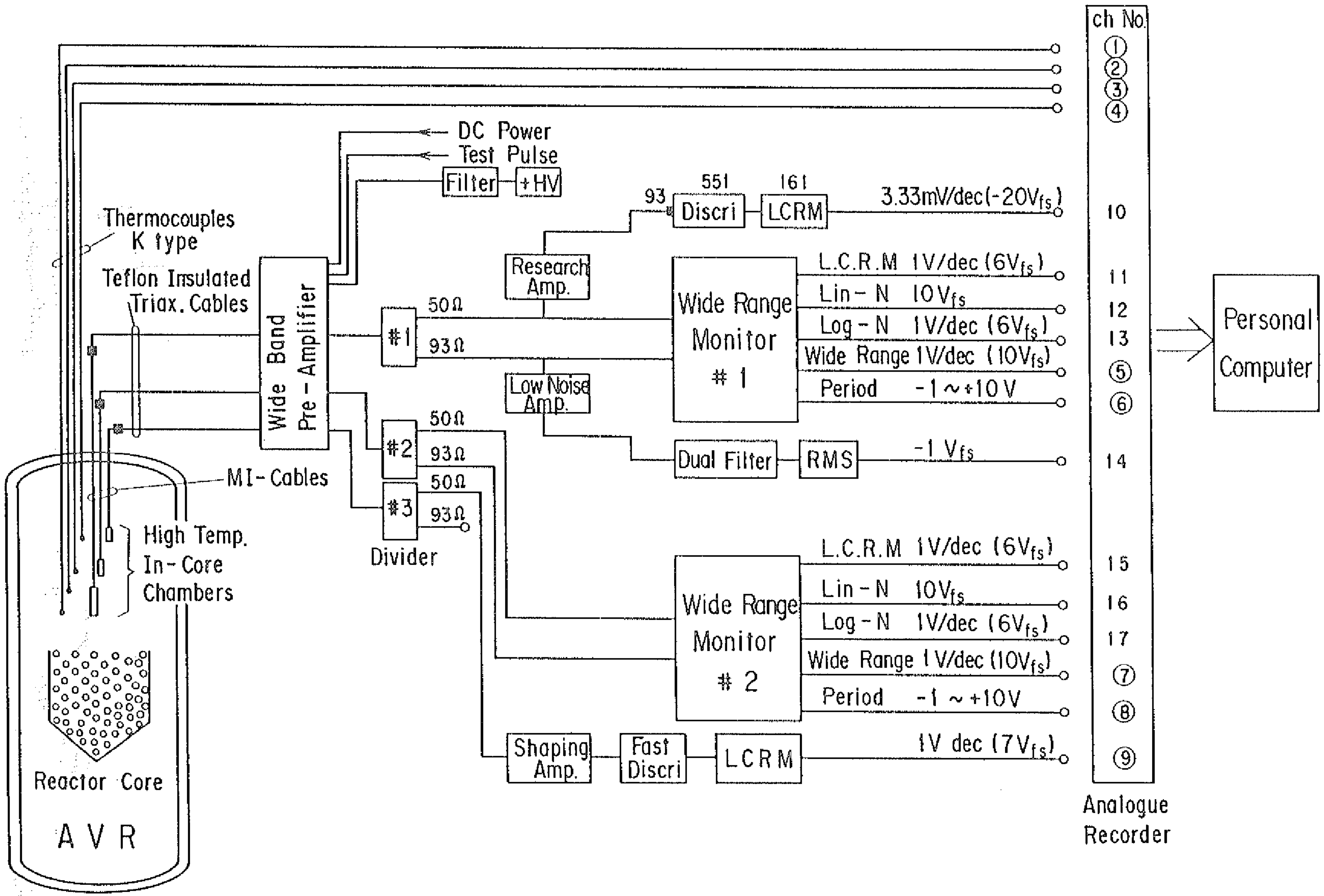

Fig. 5.1 Block diagram of Neutron Flux Measuring System for AVR experiment

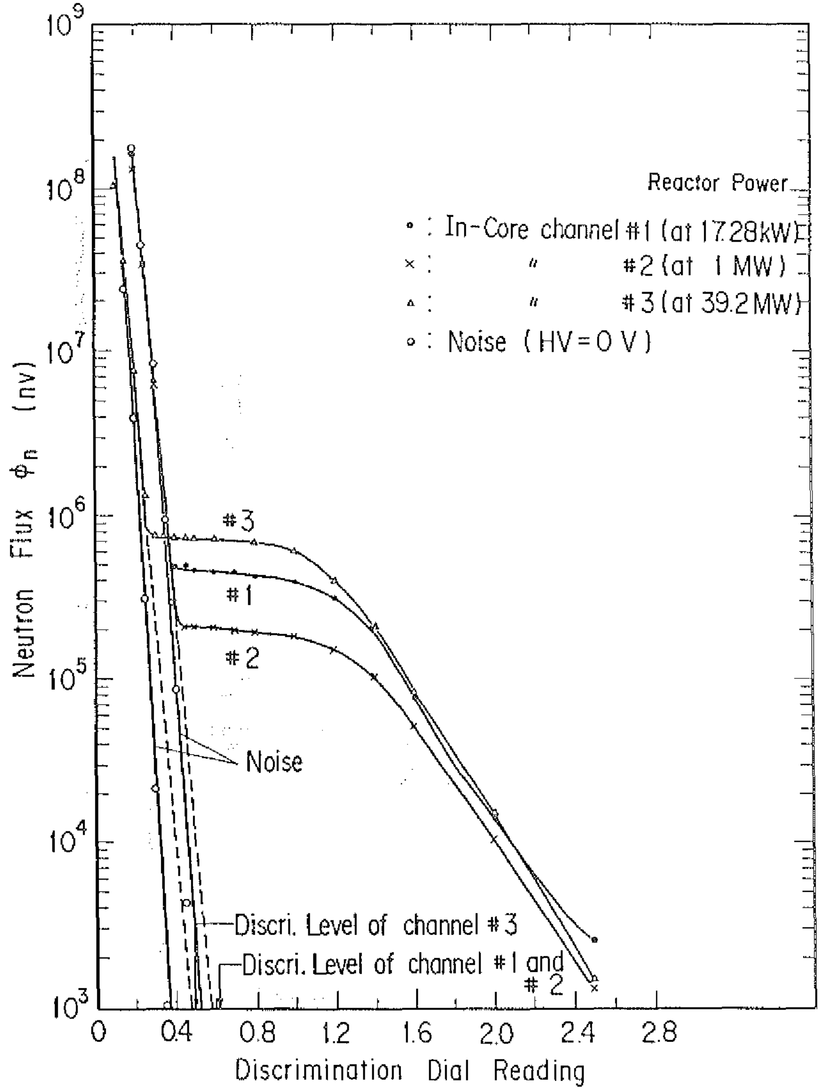

Fig. 5.2 Integral bias curves of HTICs measured in AVR

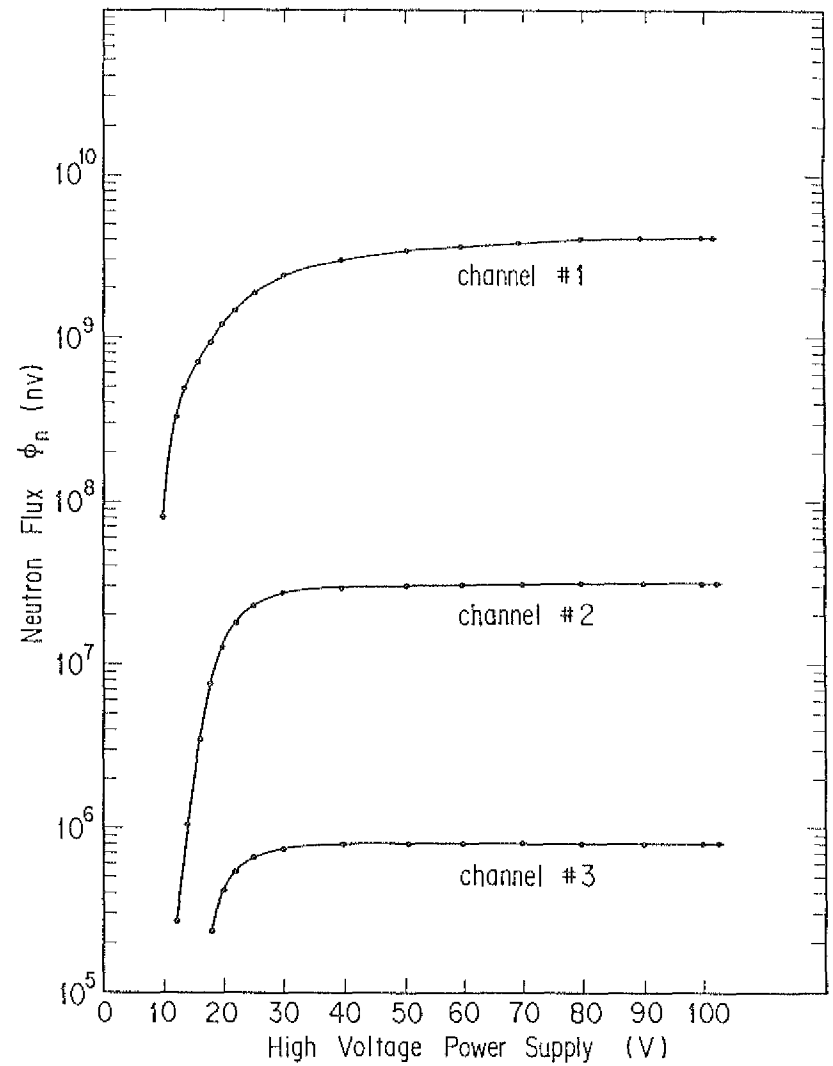

Fig. 5.3 Plateau curves of THICs measured at 42.5MW in AVR

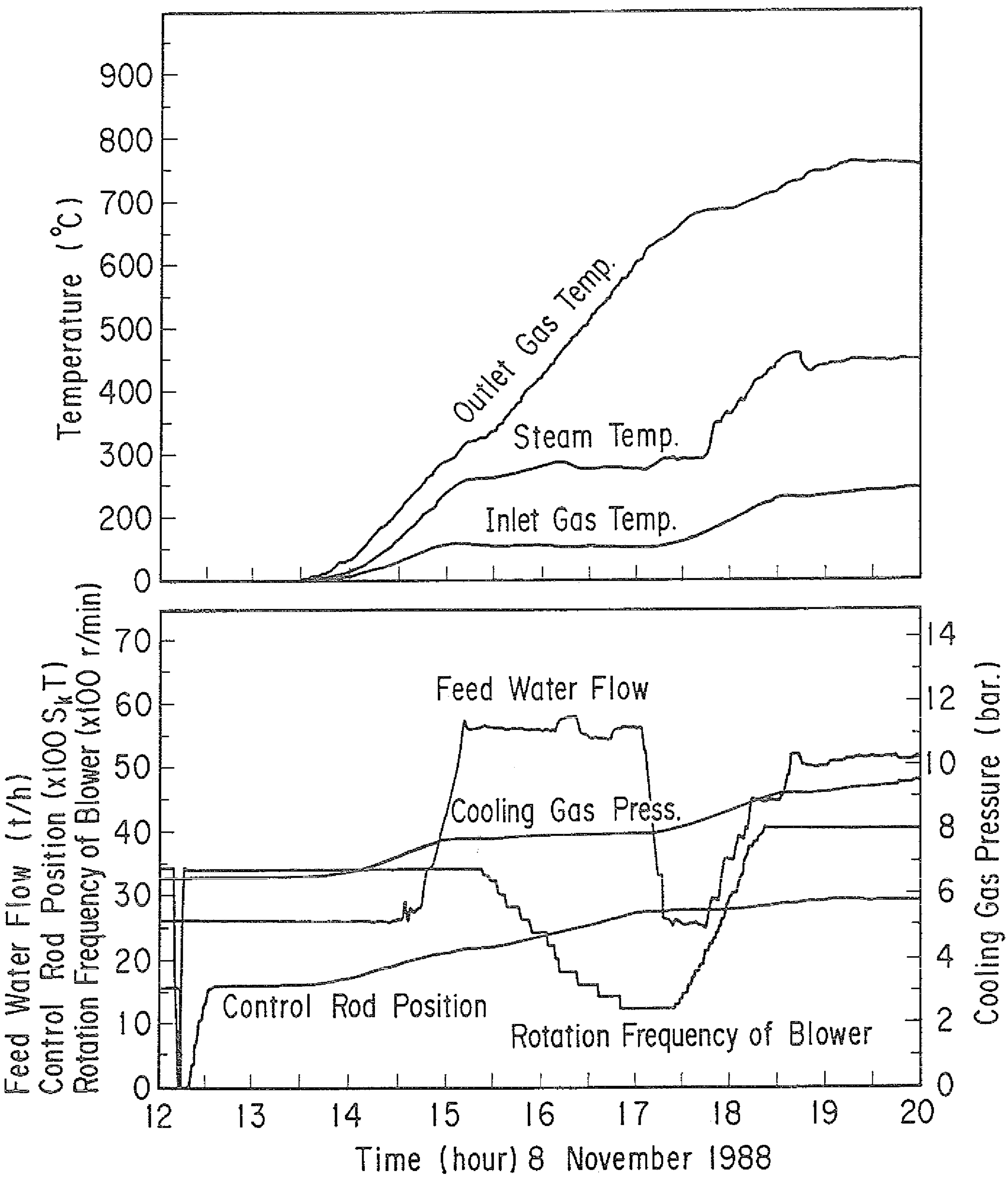

Fig. 6.1 Operation data of AVR during reactor power-up
(presented by AVR GmbH)

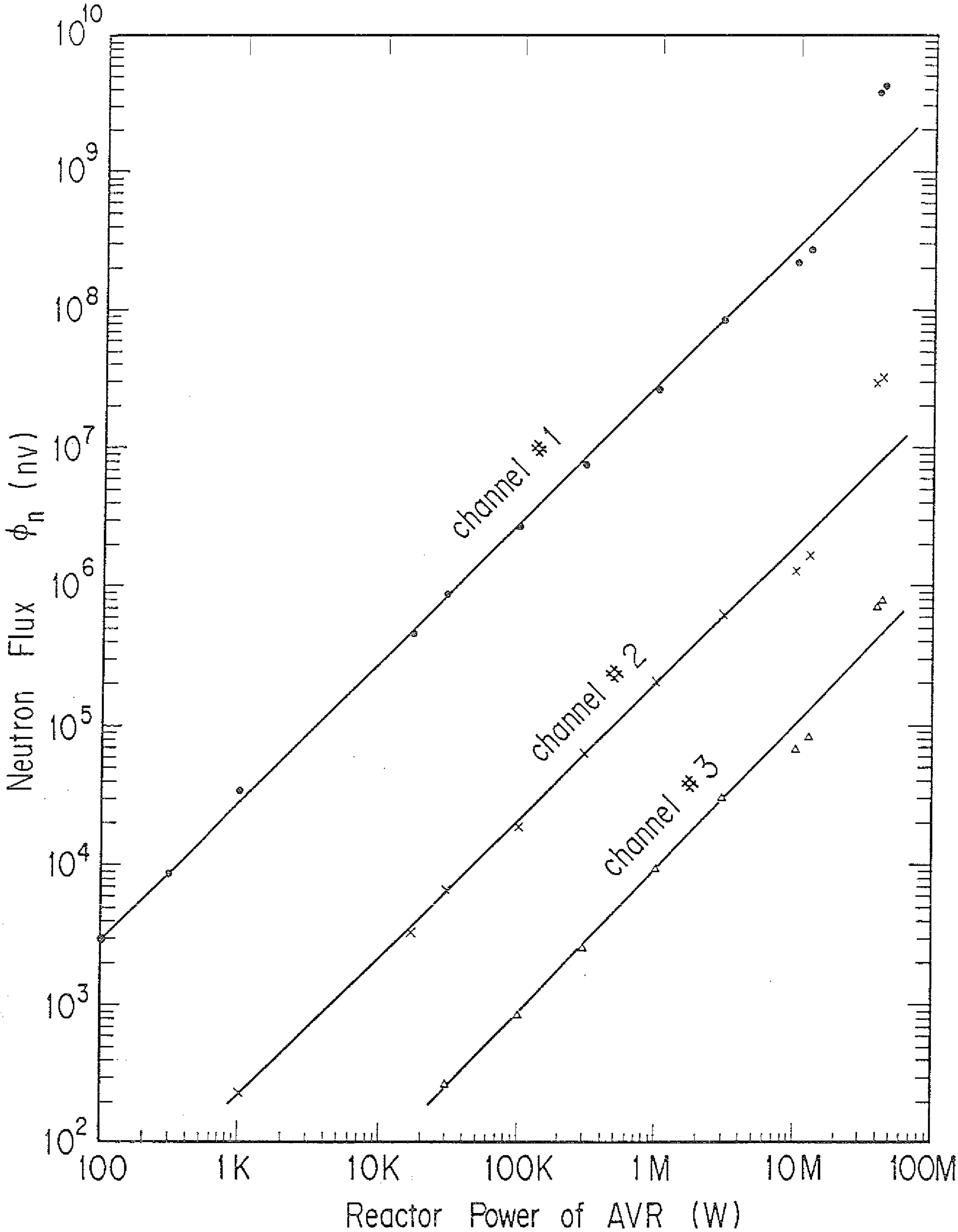

Fig. 6.2 Neutron flux in the steam generator measured at various reactor powers of AVR

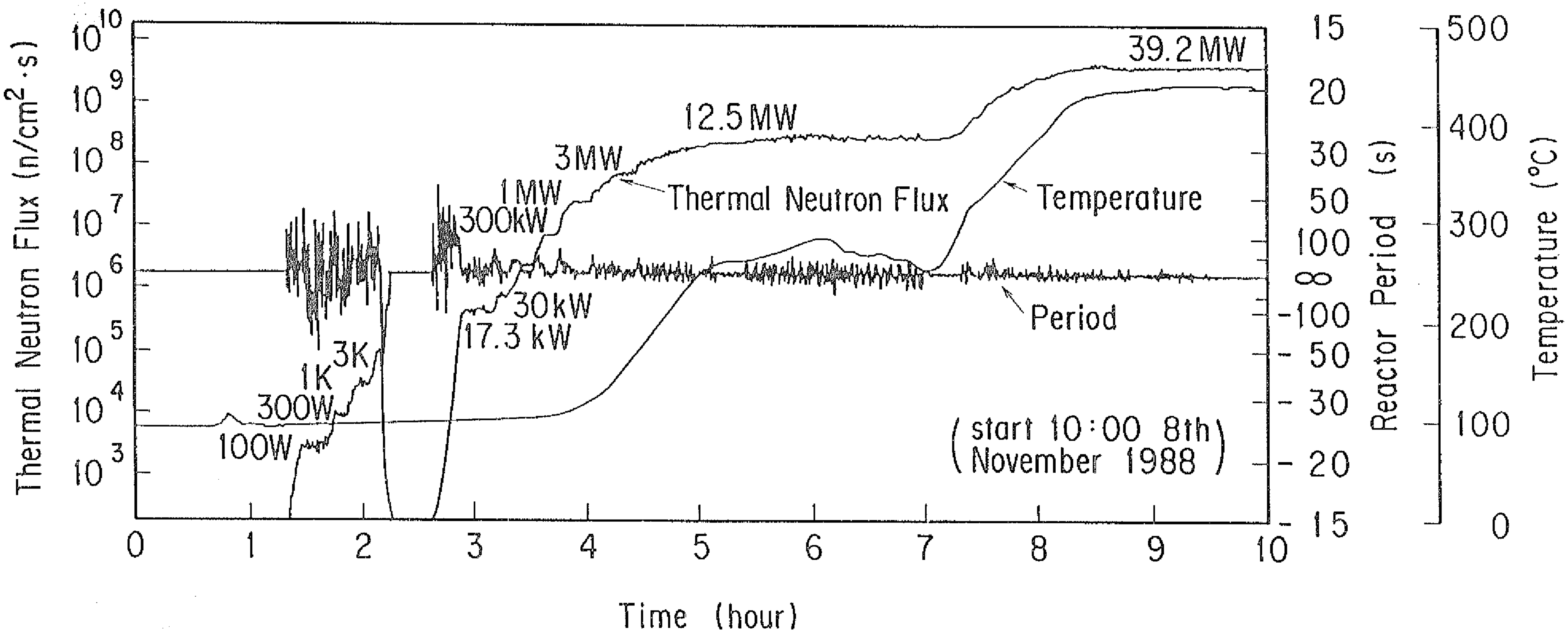

Fig. 6.3 Neutron flux and reactor period measured on real time during reactor power-up

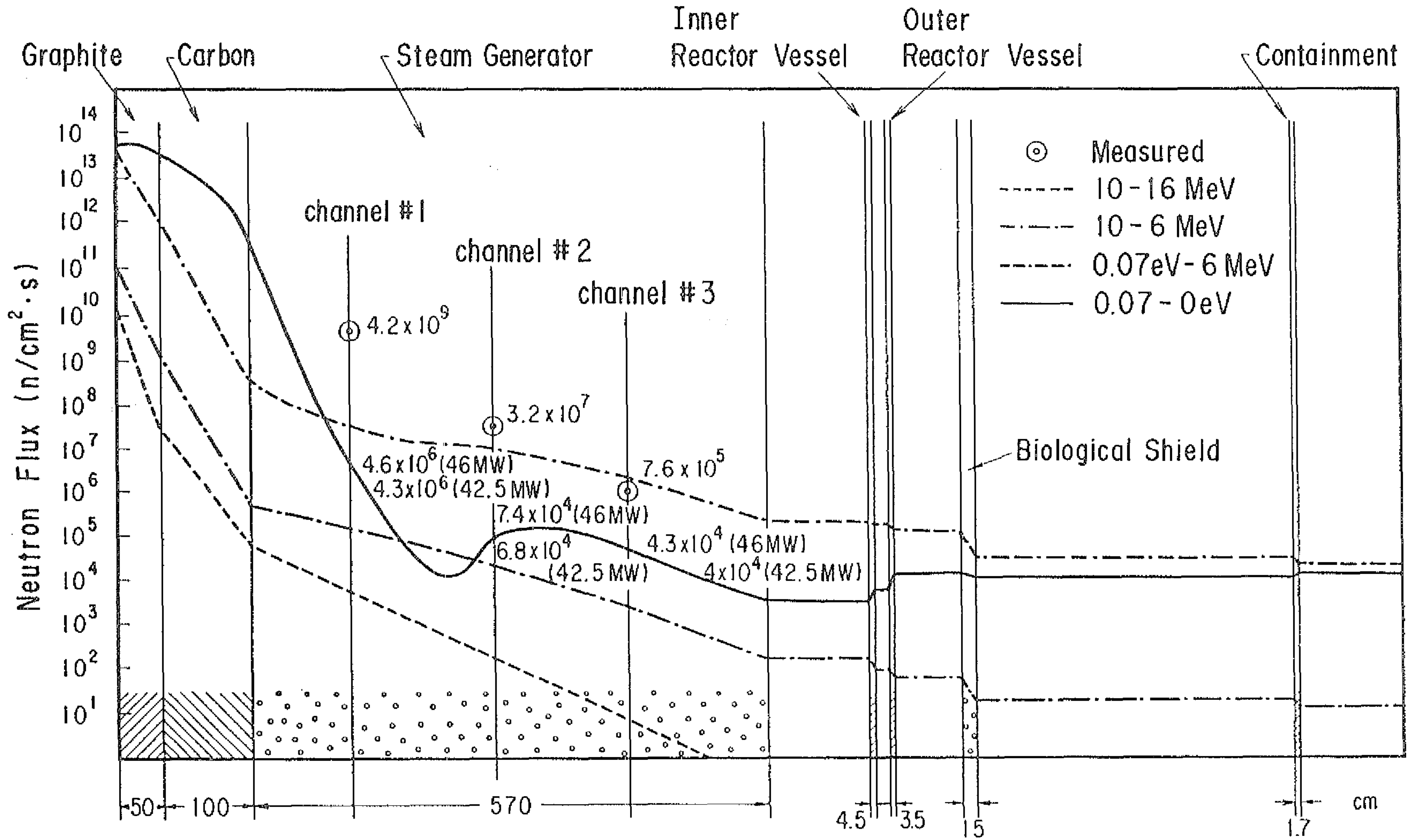

Neutron flux distribution in axial direction in AVR

Fig. 7.1 Comparison of calculated neutron flux distributions with experimental results at 42.5MW (calculated results were presented by KFA GmbH)

Table 7.1 Comparison of measured neutron flux with calculated results

Items	Ch#1 position	Ch#2 position	Ch#3 position
Measured neutron flux	$4.2x10^9$nv	$3.2x10^7$nv	$7.6x10^5$nv
Calculated results	$4.3x10^6$nv	$6.8x10^4$nv	$4.0x10^4$nv
Measured/calculated	977	471	19
Measurement position	1091mm	2646mm	4156mm
Gas temperature	443℃	337℃	299℃

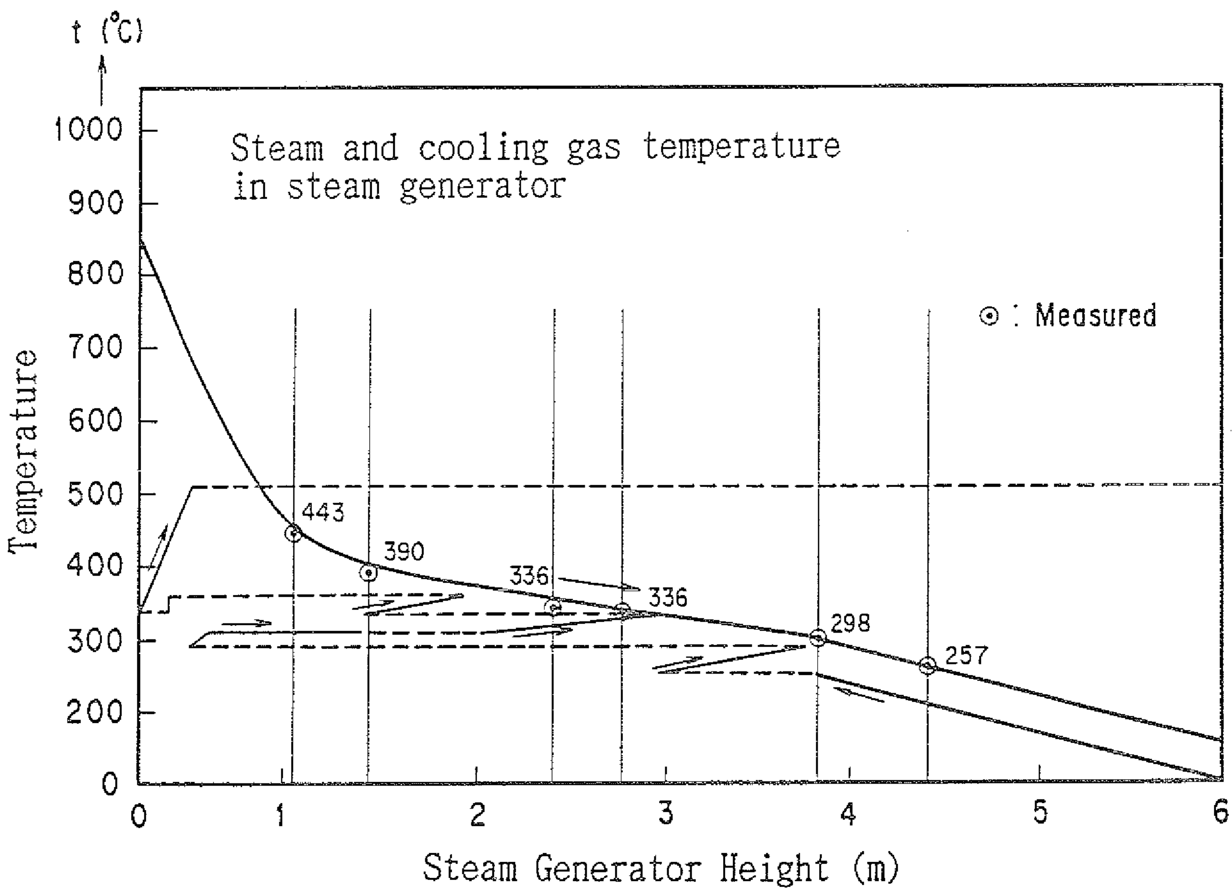

Fig. 7.2 Comparison of calculated temperature distribution with measured temperature (calculated results were presented by KFA GmbH)

FORSCHUNGSZENTRUM JÜLICH GmbH

Jül-2467
April 1991
ISSN 0366-0885